NOVA SCHOOL OF SCIENCE & TECHNOLOGY

DEPARTAMENTO DE CIÊNCIAS DA VIDA

INÊS ISABEL PEREIRA CORREIA

Licenciada em Biologia Celular e Molecular

POLYURETHANE – POLY(ETHYLENE GLYCOL) HYDROGELS FOR TISSUE ENGINEERING APPLICATIONS

MESTRADO EM GENÉTICA MOLECULAR E BIOMEDICINA

Universidade NOVA de Lisboa

Novembro, 2021

DEPARTAMENTO DE CIÊNCIAS DA VIDA

POLYURETHANE – POLY(ETHYLENE GLYCOL) HYDROGELS FOR TISSUE ENGINEERING APPLICATIONS

INÊS ISABEL PEREIRA CORREIA
Licenciada em Biologia Celular e Molecular

Orientador: Alessondra Speidel, Pós-Doutorada, Karolinska Institute Solna

Coorientador: Paula Gonçalves, Professora Associada, NOVA University Lisbon

Júri:

Presidente: Doutor Pedro Manuel Brôa Costa, Professor Auxiliar da Faculdade de Ciências e Tecnologia da Universidade NOVA de Lisboa

Arguentes: Doutora Carmen Escobedo Lucea, Investigadora Principal da Fundacion Hospital General de Valencia

MESTRADO EM GENÉTICA MOLECULAR E BIOMEDICINA

Universidade NOVA de Lisboa
Novembro, 2021

Polyurethane – poly(ethylene glycol) hydrogels for tissue engineering applications

ACKNOWLEDGMENTS

I would like to begin by thanking my supervisor, Alessondra Speidel for letting me join in on her project. Thank you for all your guidance and support, I learned a lot with you, and you gave so much confidence in the work I did. Thank you for all the patience with all the questions I asked, for always supporting and discussing with me new ideas, and above all, thank you for trusting me to do this work with you.

I would also like to thank Prof. Molly Stevens for accepting me in her laboratory and giving me such a great opportunity to learn, allowing me to spend an incredible year in Sweden with an amazing group of people.

To everyone in the Molly stevens lab, I feel very grateful for having worked alongside with you witnessing all your work, you have taught so much on what being a scientist is. Hélène, Miina, Phill, Chris, Angela, Hongya, Maggie and Anna, thank you for all your valuable input and opinions throughout my work, as well as thank you for all the fun times and for the Fika. Ilaria too, even though you only joined halfway through my journey you gave me a lot of support and I learned a lot with you, thank for keeping me company and for all the laughs.

À Nica, à Cabral e à Condez muito obrigada pelo vosso apoio, sem vocês a FCT não teria sido a mesma coisa. Obrigada por me aturarem e lidarem com as minhas crises de nervos desde BCM até agora.

À Olive, à Rosário e à Rita, obrigada por continuarem ao meu lado depois de tantos anos, vocês são as melhores.

Finalmente, Avós, Mãe, Pai, Cláudia e Aveia, obrigada pelo vosso apoio incondicional e por acreditarem sempre em mim. Obrigada por me terem dado esta oportunidade e lutarem para que eu consiga crescer e prosperar no melhor ambiente possível.

ABSTRACT

Hydrogels are one of the most common types of biomaterials in tissue engineering and regenerative medicine. In wound healing, their use has provided access to dressings that promote a faster and more effective healing, although no single dressing is able to be used in all wounds.

This work aimed at characterizing different polyurethane and poly(ethylene glycol) (PU-PEG) co-polymer hydrogel formulations and evaluating their potential as a material for wound healing. The study of the mechanical properties of hydrogels revealed a wide range of hydrogel strengths through the different formulations. Whilst no degradation was recorded in any hydrogel, their swelling profiles evidenced varied water intake within the formulations with the 12% (w/v) DABCO PU-PEG hydrogel, presenting the highest swelling ratio. Cytotoxicity assays using the L929 fibroblast cell line highlighted the hydrogels' biocompatibility. Nonfouling studies examining protein adsorption and cellular adhesion indicated that these hydrogels display a nonfouling character that is comparable to Poly(dimethylsiloxane) across all of the hydrogel formulations examined from 15% (w/v) DABCO PU-PEG to 46% (w/v) DABCO PU-PEG.

The biocompatibility of the PU-PEG hydrogels allied with mechanical properties and swelling behavior are ideal characteristics for wound dressings, as they are not only malleable and resistant to a series of strains, compatible with other materials studied for wound healing, but are also capable of exudate removal or hydration of the wound environment, promoting its healing. Furthermore, due to its nonfouling properties, a potential indication of anti-foreign body response characteristics, a desirable characteristic of biomaterials, was unveiled.

Overall, valuable characterization of the various synthesized PU-PEG hydrogels, highlighted their utility in various applications across the tissue engineering field, especially in wound healing.

Keywords: Polyurethane; Poly(ethylene glycol); PU-PEG hydrogels; Wound healing; Nonfouling; Tissue engineering

RESUMO

Hidrogéis são uma das aplicações dos biomateriais mais estudadas em engenharia de tecidos e medicina regenerativa. Na cicatrização de feridas, o seu uso tem proporcionado acesso a tratamentos que promovem uma cicatrização rápida e eficaz, apesar de um só tratamento não poder ser utilizado em todas as feridas.

Este trabalho, teve como objetivo caracterizar diferentes formulações de um hidrogel de um co-polímero de poliuretano e polietileno glicol (PU-PEG) e avaliar o seu potencial como um material para o tratamento e cicatrização de feridas. O estudo das propriedades mecânicas dos hidrogéis revelou diversas forças dos hidrogéis entre as diferentes formulações. Não se observou degradação dos hidrogéis e, os perfis de aumento de massa por absorção de água, apresentaram variações nas quantidades de água absorvida entre as diferentes formulações, sendo a mais elevada no hidrogel 12% (w/v) DABCO PU-PEG. Ensaios de citotoxicidade com a linha celular de fibroblastos L929 destacaram a biocompatibilidade dos hidrogéis. Estudos de não-incrustação (nonfouling) para avaliar a adsorção de proteínas e adesão celular indicaram o caráter nonfouling destes hidrogéis, comparável a poli(dimetilsiloxano) nas formulações de 46% (w/v) DABCO PU-PEG até 15% (w/v) DABCO PU-PEG.

A biocompatibilidade dos hidrogéis PU-PEG assim como as diferentes propriedades mecânicas e capacidade de absorção de água, tornam-nos um biomaterial com características ideais para a cicatrização de feridas visto serem maleáveis e resistentes a várias tensões, compatíveis com outros materiais estudados em cicatrização de feridas, assim como, serem capazes de remover exsudados ou de hidratar o ambiente da ferida, promovendo a cicatrização. Adicionalmente, encontrou-se, devido às suas propriedades nonfouling, um potencial efeito inibidor da resposta inflamatória a corpos estranhos, uma característica desejável dos biomateriais.

Em suma, a caracterização dos vários hidrogéis PU-PEG sintetizados, demonstra a sua utilidade em diversas aplicações na engenharia de tecidos, em especial no tratamento e cicatrização de feridas.

Palavras-chave: Poliuretano; Polietileno glicol; Hidrogéis PU-PEG; Cicatrização de feridas; *Nonfouling*; Engenharia de tecidos

INDEX

LIST OF FIGURES

LIST OF EQUATIONS

LIST OF ABBREVIATIONS

BCA	Bicinchoninic Acid
BSA	Bovine Serum Albumin
ºC	Degree Celsius
CCK8	Cell Counting Kit-8
DABCO	(1,4-diazabicyclo[2.2.2]octane)
DAPI	4',6-Diamidino-2-Phenylindole, Dihydrochloride
DBTDL	Dibutyltin Dilaurate
DMSO	Dimethyl Sulfoxide
EMEM	Eagle's Minimum Essential Medium
FBGCs	Foreign Body Giant Cells
FBS	Fetal Bovine Serum
FBR	Foreign Body Response
G'	Storage modulus
G''	Loss modulus
|G*|	Complex shear modulus
HEC	Human Epithelial Cells
ICP-MS	Inductively Coupled Plasma – Mass Spectrometry
L929	Mouse Fibroblast cell line
ms	Swollen Mass
md	Dry Mass
miw	Initial Wet Mass
md0	Day 0 Dry Mass
mw0	Day 0 Wet Mass
NC	Negative Control
P/S	Penicillin / Streptomycin
PBS	Phosphate-buffered saline
PC	Positive Control
PEG	Poly(ethylene glycol)
PDMS	Poly(dimethylsiloxane)
PU	Polyurethane
PU-PEG	Polyurethane-Poly(ethylene glycol)
ROS	Reactive Oxygen Species

rpm	Rotations per minute
RT	Room Temperature
Swiss 3T3	Mouse Fibroblasts
v/v	Volume per volume
w/v	Weight per volume

1. INTRODUCTION

1.1. Tissue engineering

Tissue engineering and regenerative medicine give rise to new ways of providing medical care. The development of these areas exploits the potential of biomaterials, cells, and other molecules to replace, repair or improve damaged tissues and organs [1-3]. Using biomaterials that are easily obtainable, to stimulate regeneration and conserve the biological function and structure of the tissues is one of the main focuses of tissue engineering in the promotion of the healing process [1,4].

The study and evolution of biomaterials has led to the development of many biomedical applications such as medical devices, biosensors, microfluidics, drug delivery devices, cell culture, tissue regeneration and wound healing [4,5].

1.2. Polymers in tissue engineering

Polymers compose a big part of the extensive research into biomaterials, and they can be of different origins [5,6].

Natural polymers, as implied, are naturally occurring materials that display great potential for biological applications. Examples of these materials are polysaccharides, such as chitosan and hyaluronan, and proteins, such as collagen and fibrin [7,8]. As these types of polymers are extracted from living systems and designated as active biomaterials, they present several advantages [3]. Since they are similar to the extra-cellular matrix, they are non-toxic, biodegradable, and highly biocompatible, promoting cell adhesion and proliferation, providing a useful platform material for cell growth and matrix production that can successfully repair and regenerate tissues [3,7]. Nonetheless, some limitations of these natural polymers include their low mechanical strength, variability between batches and difficulties in controlling degradation rates [4,5].

Synthetic polymers, like poly(caprolactone), Poly(dimethylsiloxane) (PDMS), poly(ethyleneglycol) (PEG) and polyurethane (PU) have shown considerable advantages in their use in tissue engineering due to their intrinsic characteristics [9-11]. These materials are easily synthesized, cheap, and tailorable for custom production and specific applications [3,5]. Synthetic materials are also highly reproducible, present a variety of mechanical properties and possess an inert or passive nature, meaning they do not actively participate in tissue repair and regeneration process [5]. However, even though they are not

innately bioactive, they can still instigate an immune response in the host on a higher scale compared with natural polymers due to their lower biocompatibility [3,5].

Polymeric biomaterials have varied biomedical applications as they are able to adopt diverse structures for different functions [12,13]. Many strategies have been studied to improve the characteristics of biomaterials, however, one of the most challenging aspects surrounding their use in tissue engineering continues to be overcoming the foreign body response (FBR) [5,14].

1.3. Biomaterials in tissue engineering

The implantation of any biomaterial triggers an inflammatory response in the host tissue [14]. Depending on the degree of this inflammatory reaction, it could culminate in the fibrotic encapsulation of the implanted biomaterial, preventing its interaction with the surrounding environment [12].

The process of excessive inflammation and implant failure is called the foreign body response (FBR) (Figure 1.1), and is characterized by the interaction between the host and the implanted biomaterial, leading to a series of inflammatory events that can compromise the integration and performance of the biomaterial [15].

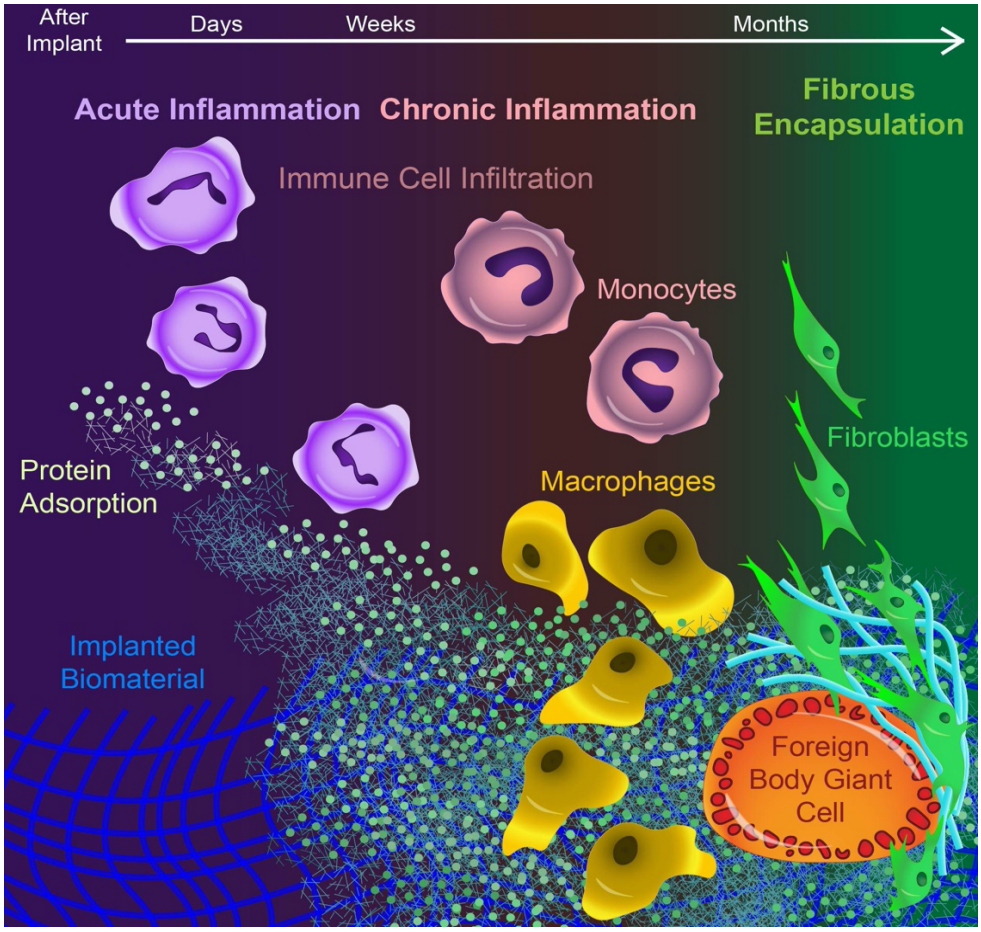

Figure 1.1 - Foreign body response to biomaterials. Scheme of the main immunological responses and events triggered once implanted biomaterials interact with the surrounding environment. Scheme made by Alessondra Speidel.

Protein adsorption onto an implanted material, also designated as biofouling, is the first step to initiate the FBR [14]. Following this, an acute inflammatory response is triggered and inflammatory cells, such as neutrophils, are attracted to the implant site by complement activation. For the first couple of days, these recruited neutrophils fight invading microorganisms and attempt to phagocytize the biomaterial, promoting cell enzymatic activity and the release of reactive oxygen species (ROS) [5,16].

Depending on the tissue damage incurred in the area surrounding the implant site can progress into a chronic inflammation phase [14]. Monocyte recruitment to the implant site, and differentiation into activated macrophages ('M1' macrophages), promotes further inflammation, with the release of proinflammatory cytokines and chemokines [16]. Macrophages then become the main cell type around the wound and continue to attempt to degrade the biomaterial by promoting the release of more ROS and enzymes as well as attempt phagocytosis of the material [5]. However, due to the size of the implant, the phagocytic process is impaired, leading to a higher release of cytokines [16]. Persistent macrophage recruitment culminates in their fusion into foreign body giant cells (FBGCs), a hallmark of the FBR [5]. The formation of the FBGCs is an attempt to increase the phagocytic activity and degradation capacity of the cells in order to destroy the implanted biomaterial [16,17]. Simultaneous to the formation of the FBGCs, macrophages shift into the 'M2' phenotype, where anti-inflammatory cytokines and pro-fibrinogenic factors are released into the site, promoting fibroblast proliferation [5,16]. Around 28 days after implantation, the activated fibroblasts increase collagen synthesis to aid tissue regeneration and wound healing, however due to the elevated number of activated cells, the production of collagen becomes excessive, prompting fibrotic deposition, and consequently forming a fibrotic capsule around the biomaterial, preventing its interaction with the surrounding environment [15].

Although the FBR can be a beneficial event as it is a protective response of the body against foreign and possibly harmful materials, it can be detrimental for effective implant function [14]. The duration of the FBR is dependent on various factors, one of them being the size and properties of the biomaterial [16]. Thus, choosing a material that has an ability to moderate the FBR can encourage a better tolerated implant [12].

1.4. Commonly used biomaterials

PDMS is a type of polymer-based silicone broadly used in medical devices and surgical implants [11,18]. This material is desirable for these applications due to its biocompatibility, non-toxic and inert character, elastomeric properties, low cost and the fact that it is easily fabricated [18,19]. Nonetheless, PDMS can present some drawbacks in implantation applications, such as biofouling of non-specific proteins which can consequently promote undesired cell attachment and trigger immune responses such as the FBR. Thus, several approaches have attempted to address PDMS' biofouling nature and biocom-

patibility, such as introduction of surface coatings [19-21] or changes in topography and roughness, as recently certain surface topographies of silicone breast implants have been shown to provoke a higher immune response, FBR [22].

One other commonly used polymer is PEG. This material is biocompatible, non-toxic, hydrophilic and biodegradable [23]. Due to its hydrophilicity, PEG is able to reduce biofouling, thus, it has been studied as a material for coating other devices and materials to reduce non-specific protein adsorption [17,18]. One of PEG's main applications is towards the synthesis of three-dimensional polymeric and hydrophilic hydrogels, characterized by a porous network and high-water content giving them the advantage and capacity to be used as a vehicle for drug delivery and wound dressings [24,25]. In wound healing PEG is able to provide solutions that display a good performance in both wound closure and bleeding control [26], promoting healing and inhibition of cell growth whilst producing biocompatible degradation products [27].

Polyurethane (PU) is another synthetic polymer whose mechanical properties, biocompatibility, non-toxicity and biodegradability support its use in tissue engineering [6]. This polymer has been studied for various applications from wound healing and drug delivery [28,29] to an implantable substrate for plastic surgery [30] along with other biomedical applications [13]. PU is a polymer often used in wound healing as a semi-permeable wound dressing, and is characterized by its elastic and flexible behavior, allowing it to be easily adaptable to the damaged sites [9,31].

Co-polymers have also become a source of interest as they can improve the initial materials' properties [5,6]. Both PEG and PU have been studied together for several applications in tissue engineering and biomedicine [32,33]. One of their most studied applications is towards the production of hydrogels, whose mechanical and swelling properties as well as biocompatibility are favorable for biomedical applications [32]. The incorporation of PEG into the PU network, enables the production of a hydrogel that can present a non-fouling character, exhibiting low protein adsorption and cellular adhesion, due to an increase in material hydrophilicity, characteristic of the PEG polymer [34]. Several applications of these PU-PEG hydrogels have been studied as potential drug delivery vehicles [35] and as coatings to improve materials biocompatibility [36]. This co-polymer hydrogel has also been studied for wound healing where its high potential as a dressing was evidenced by providing an ideal moist environment and promoting desirable epithelization [37].

1.5. Biomaterials in Wound healing

Wound dressings have become a major application of biomaterials, where they are explored for promoting a faster and more effective wound healing process [13].

Wounds, depending on their cause and healing time, can be designated as either acute or chronic. Acute wounds usually occur due to accidents, surgical injuries or burns, and the wound healing process they undergo is considered the usual course. Chronic wounds, such as ulcers, are characterized by an

impaired healing process, and full recovery is not possible, being often associated with pre-existing comorbidities, such as diabetes or other infections [38-40].

Wound healing is a continuous and dynamic process characterized by four sequential phases [38,41,42]. The first phase is hemostasis where, following injury, vasoconstriction and platelet aggregation occur to prevent blood loss and a fibrin clot is formed, promoting the release of pro-inflammatory cytokines and growth factors [25,41]. This release recruits inflammatory cells and begins the second phase called inflammation, where both neutrophiles and macrophages are present to clear away pathogens, endogenous materials and debris. Lymphocytes are also recruited and differentiate into macrophages in the later stage to further continue their functions and begin formation of granulation tissue and stimulate fibroblast activity [39,41,42]. The proliferative phase then follows, where active fibroblasts produce collagen, angiogenesis is initiated, granulation tissue continues to form, and epithelial cells proliferate and migrate, promoting re-epithelization and wound closure [41,42]. The final phase is designated resolution or remodeling, consisting of capillary regression, recovery of tissue architecture due to collagen turnover and wound contraction caused by myofibroblasts [39,41,42].

Wound dressings, when first developed, introduced the creation of a protective barrier against the external environment and the action of microorganisms [25,40]. Some of the most used traditional dressings are gauzes and bandages, and although affordable and effective, they tend to create a dehydrated environment due to evaporation of wound exudate, attaching to the wound, and not creating the ideal conditions for accurate healing [40]. Thus, optimal wound dressings should be able to ensure that an ideal environment is created, keeping it moist, as it has been shown that it enables faster epithelization when compared to wounds that are dry or exposed to air [43]. In addition, they should favor oxygen circulation, help molecular and cellular bioprocesses, such as the formation of new blood vessels and cell proliferation, and be occlusive to keep the wound not only moist but free from pathogens and external stresses [7,9].

The development of modern wound dressings, such as films, foams, hydrocolloids and hydrogels, has been growing with the application of different materials and varied formats to aid and stimulate wound healing and tissue regeneration [44].

1.5.1. Hydrogels in wound healing

Hydrogels are one of the most promising wound dressings, as they provide the desired moisture in the wound environment, optimal for healing and confer a barrier to protect against infection [25,44]. Hydrogels contain an elevated water content which keeps the wound hydrated and cool [31]. Exudates from the wound can also be removed by the hydrogels, however, this characteristic is limited to wounds that are either dry, necrotic, or moderately exuding [40]. Hydrogel dressings are usually transparent, allowing easy observation of the healing progress, and are easily applied and removed without further damage [31,39].

The application of hydrogel dressings can promote wound healing in a passive or active way due to their intrinsic characteristics such as swelling and degradation behavior. Both these characteristics can contribute to a controlled release of active biomolecules through time, such as drugs or wound healing components, promoting faster wound healing and cell growth in the damaged site [45]. Currently there are several hydrogels and hydrogel-based wound dressings already commercially available [25,31]. Nonetheless, some disadvantages are still associated with the use of hydrogels, such as the low material strength and exudate accumulation leading to maceration and bacterial infection [31].

The variety and necessities of each wound does not allow for one material to fit the specifications required for all types of wounds [39], thus novel studies and ideas are constantly needed to innovate and provide distinct ways to promote wound healing.

1.6. **Aims**

Although materials might be useful for a wide range of applications, this work was focused on the discussion and analysis of a possible application in a wound environment.

The aim of this work is to characterize different formulations of polyurethane and poly(ethylene-glycol) (PU-PEG) hydrogels cast in a novel setup, using western blot glass plates, and evaluate their potential use as a biomaterial for wound healing, in tissue engineering.

Already synthesized PU-PEG hydrogels, adjusted to a single step synthesis [35], will be characterized by determining their mechanical properties using rheology to measure frequency and strain sweeps, as well as by measuring the swelling behavior and hydrogel degradation. Hydrogel cytotoxicity will be assessed with a fibroblast cell line (L929) to evaluate the impact of the substitution of the catalyst, from a tin containing catalyst dibutyltin dilaurate (DBTDL) to an organic catalyst 1,4-diazabicyclo[2.2.2]octane (DABCO), together with the casting set-up used. Evaluation of blue food coloring toxicity will also be determined directly on cells or when incorporated in hydrogels, to assess if it could be a good marker for implant recovery. Protein adsorption of albumin and fibrinogen, two highly abundant blood proteins, and cell adhesion to the surface of the PU-PEG hydrogels will also be determined and compared to a widely used biomaterial, PDMS.

By profiling the various characteristics of the various formulations of the PU-PEG hydrogels, the materials will be evaluated as potential wound healing dressings as well as a platform material with a wide number of possible applications in tissue engineering/regenerative medicine.

2. MATERIALS AND METHODS

2.1. Polyurethane - Poly(ethylene glycol) Hydrogels

All polyurethane – poly(ethylene glycol) (PU-PEG) hydrogels used throughout the work were kindly synthesized by the chemists in the laboratory. 46%, 23%, 18%, 15% and 12% (w/v) PU-PEG hydrogels were synthesized using an organic catalyst 1,4-diazabicyclo[2.2.2]octane (DABCO) or dibutyltin dilaurate (DBTDL) [35] and dimethyl sulfoxide (DMSO) (Figure 2.1 A-C). For the 23% (w/v) DABCO PU-PEG hydrogels, two casting set-ups were used: a flat one, cast between two western blot glasses, and a vial one, with a cylindrical shape (Figure 2.1D).

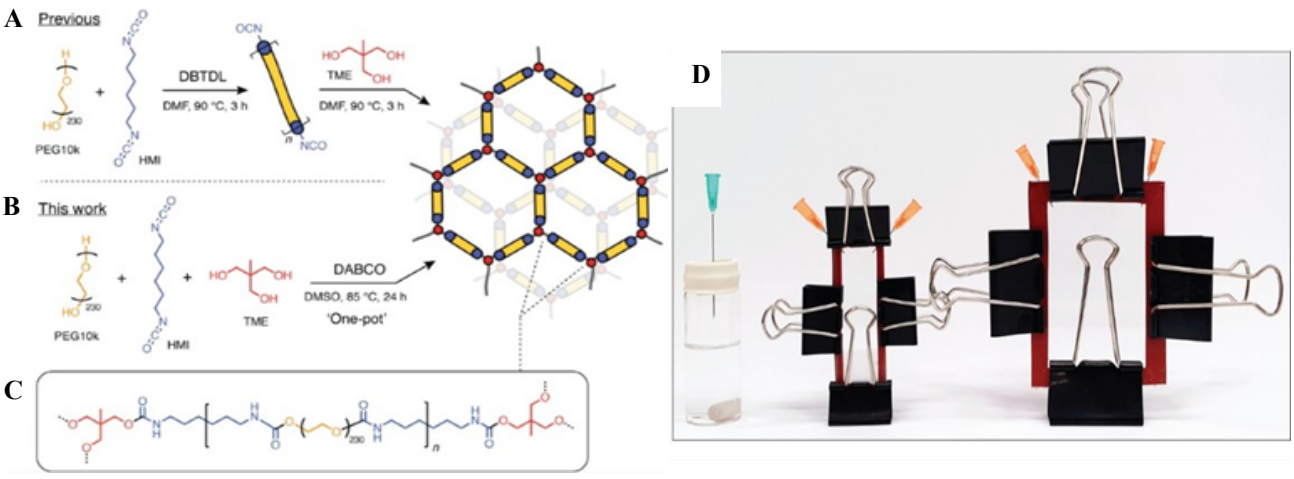

Figure 2.1 - Polyurethane and poly(ethylene glycol) hydrogel synthesis chemistry and casting set up. (A) Synth process using dibutyltin dilaurate (DBTDL) as a catalyst. (B) Synth process using 1,4-diazabicyclo[2.2.2]octane (DABCO) as a catalyst. (C) Hydrogel chemical structure. (D) Vial cast (on the left) and Western blot glasses set up (center and on the right) for Flat cast. Images courtesy of Alessondra Speidel.

2.2. **Hydrogel Rheology**

To evaluate the hydrogels' mechanical properties and overall resistance to forces, rheology was performed on an AR 2000EX Dynamic Shear Rheometer (TA instruments, Newcastle, Delaware, United states of America (USA)). For each sample studied, at least 3 samples with 8 mm diameter were cut using a hole puncher (JLB320cm, BOEHM, Sweden). Using the Rheology Advantage Software, both frequency and strain sweeps were measured at 22,5°C. Frequency sweep measurements were performed with frequency values ranging from 1 to 100 rad/s and fixed strain at 0,01 (1%). The strain sweeps were measured using a fixed frequency value of 10 rad/s with a range of strain values from 0,2% to 100%. One at a time, each gel was placed in the rheometer and aligned between the plate and piston, and the gap for the gel was set followed by the measurements of the storage (G'), loss (G'') and complex shear (G*) modulus for both frequency and strain sweeps. At least three replicate hydrogel samples were analyzed for at least three independent syntheses of each hydrogel formulation studied.

2.3. **Degradation and Swelling Studies**

For the study of swelling and degradation of PU-PEG hydrogels, 10 mm diameter discs were made for all formulations, and the mass of each sample was measured on an electronic balance (SECURA224-1S, Satorius Lab instruments, Germany) and distributed into groups of three gels for each of the five time points so that there was no significant difference in average starting mass. After hydrogel preparation, a picture of a representative sample (median wet mass sample) for each group was taken, and all samples were individually placed in a histology plastic cassette. Day 0 samples were put in dry ice for 1 h and after left in the freeze drier (Labconco, Kansas City, MO, USA) overnight, applying vacuum according to manufacturer's instructions. The remaining 4 groups of samples corresponding to days 1, 7, 14 and 35 were placed in a beaker with ultrapure water (Milli-Q® Direct, Merck Milipore, Sweden) (~800mL) already equilibrated at 37ºC in a warm bath (isotemp GPD28, ThermoFisher Scientific, Waltham, Massachusetts, USA), and at each timepoint their swollen masses (ms) were recorded and then left to freeze-dry overnight, whilst the remaining samples were transferred to a new beaker with fresh ultrapure water (~800mL) and left in the warm bath. Once dry, the hydrogel discs' mass was measured (md), and a picture of the representative sample was taken. The swelling ratio of each hydrogel was measured by dividing the gels' swollen mass by their dry mass (Equation (2.1)). Hydrogel degradation was measured by first calculating the expected dry mass of each sample by multiplying the initial wet mass of each individual sample (miw) with a ratio of averaged day 0 dry mass (md0) and day 0 wet mass (mw0) (Equation (2.2)). Mass loss was then obtained by removing each individual sample dry mass from the expected one dividing by the expected dry mass (Equation (2.3)).

$$\boldsymbol{Swelling\ Ratio} = \frac{ms}{md} \qquad \text{Equation (2.1)}$$

$$\textbf{\textit{Expected Dry Mass}}\ (mg) = miw\ x\ \left(\frac{md0}{mw0}\right) \qquad \text{Equation (2.2)}$$

$$\textbf{\textit{Mass Loss}}\ (\%) = \frac{(Expected\ Dry\ Mass - md)}{Excpected\ Dry\ Mass}\ x\ 100 \qquad \text{Equation (2.3)}$$

All determined values were obtained from 3 different synthesis for each formulation, using the averages of at least 3 samples from each run.

2.4. L929 fibroblast cell culture

The mouse fibroblast cell line (NCTC clone 929 [L cell, L-929, derivative of Strain L] ATCC® CCL-1TM) was maintained in EMEM (ATCCTM, Manassas, VA, USA) completed with 10% (v/v) of fetal bovine serum (FBS, Gibco™, Göteborg, Sweden) and 1% (v/v) of penicillin/streptomycin (P/S, Gibco™, Göteborg, Sweden) at 37ºC with 5% of CO_2. Cells were passaged every 2 days. All assays were performed when the cells were at around 80% confluency. For catalyst and casting set-up cytotoxicity experiments cells at passage 11 were used, and for cell adhesion experiments cells at passages 10 and 11 were studied.

2.5. Sample sterilization

To prepare for cell culture, PU-PEG hydrogels and polyethylene tubing (Becton, Dickinson and company, New Jersey, USA) after cut, were washed twice with 35 mL of absolute ethanol (Fisher Scientific, United Kingdom (UK)) for 1 h at RT in a roller (Tilt/roller mixer SRT 6D, Stuart, Sweden) at 60 rpm. Followed by six more washes with 30 mL of autoclaved ultrapure water for 1 h each at 60 rpm RT, to remove any remaining ethanol content.

2.6. *In vitro* cytotoxicity study

2.6.1. Sample preparation

2.6.1.1. Catalyst and casting set-up impact on cytotoxicity

Hydrogel samples were cut into 3 mm diameter discs from the 23% (w/v) DABCO PU-PEG samples that either contained the DBTDL or DABCO catalyst, from both casting formats. The mass of each sample was based on its extraction ratio, together with each gel swelling ratio, assuming 19.6 for DABCO and 12.7 for DBTDL samples, to account for any swelling. After hydrogel sterilization, the samples were freeze dried to remove any remaining liquid in the samples, and then placed in EMEM for material extraction, according to section 2.6.2.

2.6.1.2. Blue food coloring cytotoxicity

Blue food coloring (Dr. Oetker, Bielefeld, Germany) was considered for marking hydrogels for simpler post-implantation localization. The blue food coloring solution (stock at 0.74% (w/v)) is composed of water, brilliant blue (E 133), citric acid (E 330), sodium benzoate (E 211) and potassium sorbate (E 202). Cytotoxicity of the food dye was assessed by using different concentrations: 0.77% (w/v), 0.385% (w/v), 0.1295% (w/v) and 0.077% (w/v) of blue food coloring. 6 mL of the blue food coloring stock solution were lyophilized, and based on its dry mass, EMEM was added to reach the desired final concentrations of the food dye, according to section 2.6.2.

2.6.1.3. Cytotoxicity of hydrogels embedded in blue food coloring

The cytotoxicity of blue food coloring stained 46% (w/v) DABCO PU-PEG hydrogels was also assessed. Sterile hydrogel (3 mm diameter) discs were incubated at RT in 5 mL of either filter sterilized blue food coloring (0.74% (w/v) of blue food coloring) or in ultrapure water. After 48 h, both ultrapure water and blue food coloring were removed, and the samples' masses were obtained to determine the volume of EMEM to add as described in section 2.6.2.

2.6.2. Cytotoxicity test procedure

For *in vitro* cytotoxicity studies, polyethylene tubing (3 mm long) and citric acid (Sigma-Aldrich, Sweden) were used as the negative and positive controls, respectively. Together with these controls, complete medium and tissue culture plastic (wells containing medium alone) were used as internal controls. After sterilization, polyethylene tubing was left 1 h in dry ice and then freeze dried according to manufacturer's instructions. Following the preparation of the different samples as detailed in section 2.6.1.1 through section 2.6.1.3, EMEM was added at 89% (v/v) to all conditions according to ISO standard (ISO 10993-5) extraction rates for each sample: 1 mL of EMEM per 8,484 mg of Citric acid and 1 g of hydrogel, polyethylene tubing or blue food coloring per 5 mL of complete media, and the samples were incubated for 24 h in a shaking incubator at 125 rpm at 37ºC. L929 cells were seeded on a 96-well plate at 94000 cells/mL and pre-cultured for 24 h with 100 µL of complete medium (EMEM with 10% (v/v) FBS and 1% (v/v) P/S) at 37ºC with 5% of CO_2. Media was extracted from the various material-treated set-ups through collection with a syringe and needle, and filter sterilized using a 0,2 µm filter (WhatmanTM, GE healthcare, UK). Extracted media was then complemented with addition of FBS and P/S to reach final concentrations of 10% and 1% (v/v), respectively. The cells' media was replaced with the extracted media, followed by incubation at 37ºC with 5% of CO_2 for 24 h and 72h. The cell metabolic activity was determined using Cell Count Kit - 8 (Sigma-aldrich, St. Louis, Missouri, USA) according to manufactures instructions. Briefly, after 3 hours of incubation with the CCK-8 reagent at 37ºC with 5% of CO_2 the absorbance was measured on a Varioskan™ LUX multimode microplate reader (Thermo

Fisher Scientific, Waltham, Massachusetts, EUA) at 450 nm. Absorbance values for all experimental samples were normalized to the negative control for each repeat (at least 3) of the experiment.

The pH of the extracted media from all experimental samples was measured. The readings were performed using either Mettler Toledo™ FiveEasy Plus™ FEP20 pH Meter (Fisher Scientific, Sweden) or pH indicator test strips (VWR, Sweden) when sample volume was low.

2.7. **Hydrogel protein adsorption**

Protein adsorption of the PU-PEG hydrogels was studied through a Bicinchoninic Acid (BCA) assay using both albumin and fibrinogen, both found in blood at high concentrations. The hydrogel samples were compared against a highly used biomaterial in medical devices, Polydimethylsiloxane (PDMS) (SYLGARD® 184 Elastomer Kit, VWR, Sweden). Based on the rheological profile of PDMS, the reagents proportions of base agent and curing agent were determined 50:1, respectively, to match shear moduli of the 23% (w/v) PU-PEG hydrogels [46,47]. A calibration curve, to help determine the concentration of adsorbed proteins by the PU-PEG hydrogels, was designed with 46% (w/v) DABCO PU-PEG gels, adapted from the PierceTM BCA Protein Assay Kit (Thermo Scientific, Waltham, Massachusetts, USA) with bovine serum albumin (BSA, Thermo Scientific, Waltham, Massachusetts, USA) and bovine plasma fibrinogen (EMD Milipore, Germany) standards at 1500 µL/mL, 1000 µL/mL, 750 µL/mL, 500 µL/mL, 250 µL/mL, 125 µL/mL, 50 µL/mL, 25 µL/mL, 5 µL/mL and 0 µL/mL. Discs of 6 mm diameter were cut from different hydrogel samples and left incubating overnight in 1X Phosphate-buffered saline (PBS, Gibco™, Göteborg, Sweden). 25 µL of albumin or fibrinogen standards of the various calibration curve concentrations were added to hydrogel samples for the calibration curve. Experimental samples form 46% (w/v) DABCO PU-PEG, 23% (w/v) DBTDL PU-PEG, 23% (w/v) DABCO PU-PEG, 18% (w/v) DABCO PU-PEG, 15% (w/v) DABCO PU-PEG and 12% (w/v) DABCO PU-PEG hydrogels were incubated in a fresh solution of 1 mg/mL bovine serum albumin in PBS or 4 mg/mL bovine plasma fibrinogen in PBS for 2,5 h. The experimental samples were washed three times with PBS for 1 min each and afterwards the BCA assay proceeded according to manufacturers' instructions. After cooling down for 15 min, the absorbance was measured using the Varioskan™ LUX multimode microplate reader at 562 nm.

2.8. **Biofouling assay**

A biofouling assay was conducted to evaluate the non-fouling potential of the synthesized hydrogel formulations in comparison to PDMS. For this study 3 to 5 hydrogel discs of 6 mm diameter from at least 3 syntheses of 46% (w/v), 23% (w/v), 15% (w/v) and 12% (w/v) DABCO PU-PEG hydrogels and PDMS (50:1) were used. The discs were sterilized with 35 mL of 70% (v/v) Ethanol (TechniSolv®, VWR, Sweden) and then washed 5 more times with 30 mL of autoclaved ultrapure water, and twice with completed EMEM for 30 min at 37ºC, with 5% of CO_2. L929 cell were seeded at 48000 cells/mL

on each hydrogel surface and left to attach for 24 h at 37ºC with 5% of CO_2. After incubation, the samples were washed gently with 150 µL of 1X PBS, followed by fixation with 150 µL 4% Paraformaldehyde (Histolab®, Sweden) for 15 min at RT. Once fixed the samples were washed with 150 µL 1X PBS and left overnight 4°C. The samples were washed two more times with 150 µL of 1X PBS for 1 min, followed by the addition of 150 µL of 0.1% Triton™ X-100 (Sigma - Aldrich, Sweden) in PBS for 5 min. After three more washes with 1X PBS for 5 min each, the samples were stained with 300 nM of 4',6-Diamidino-2-Phenylindole, Dihydrochloride (DAPI, Life technologies, Sweden) in a 1% (w/v) BSA in PBS solution for 20 min at RT, inside a covered container. The samples were washed three times with 1X PBS (5 min each) and after were scooped from the wells and added to a microscope slide for imaging with the ZEISS Axio Imager 2 (ZEISS, Sweden). Cells were counted according to DAPI signal observed at 470 nm, by either counting directly from the microscope upon observation dividing by the entire surface area of the hydrogel, or by counting afterwards from the images obtained using Fiji (Version 1.0) dividing by the area of each counted square.

2.9. **Data analysis**

Results are given as mean ± standard deviation. Statistics of the obtained data was accessed using GraphPad PRISM (Version 9.2.0 (283)) with post hoc one-way ANOVA test and Tukey's multiple comparisons or unpaired t-test. Values with p-value less than or equal to 0.05 were considered statistically significant. Calibration curves were obtained with Microsoft Excel.

3. RESULTS

3.1. Hydrogel rheology

To study material deformation in response to a force, rheology was conducted on the different hydrogel formulations (from flat casts). One representative frequency sweep from each sample studied was plotted (Figure 3.1), displaying both storage modulus (G') and loss modulus (G''), that correspond to the hydrogels solid and liquid behavior, respectively.

No impact in G' was found with the increase in frequency, with values remaining constant. However, fluctuations in G'' at frequencies above 10 rad/s were present. Until a frequency of 10 rad/s, the material suffered no disturbances in its elastic components (Figure 3.1).

The characterization of hydrogel behavior at different strain values, was conducted by a strain sweep with a fixed frequency of 10 rad/s, between 0.001 and 1 strain. One representative sweep is displayed from each gel in figure 3.2A. The hydrogels' behavior was independent of strain below 0.01 strain for 46% (w/v) DABCO PU-PEG, 0.02 strain for 23% (w/v) DBTDL PU-PEG, 23% (w/v) DABCO PU-PEG and 15% (w/v) DABCO PU-PEG, 0.07 strain for 18% (w/v) DABCO PU-PEG and 0.30 strain for 12% (w/v) DABCO PU-PEG.

The hydrogels' overall resistance to forces was determined when the strain was at 0.005 (Figure 3.2A traced line and 3.2B), and it was observed that the highest PU-PEG concentration (46% (w/v) DABCO PU-PEG) had the greatest complex shear modulus (|G*|) value. The average |G*| of 46% (w/v) DABCO PU-PEG was 28249 ± 11053 Pa, 10839 ± 4939 Pa for 23% (w/v) DBTDL PU-PEG, 7717 ± 5800 Pa for 23% (w/v) DABCO PU-PEG, 4907 ± 4081 Pa for 18% (w/v) DABCO PU-PEG, 2598 ± 2572 Pa for 15% (w/v) DABCO PU-PEG and 1716 ± 1898 Pa for 12% (w/v) DABCO PU-PEG hydrogel samples. Within the range of concentrations studied, a very significant difference in resistance to forces was found between both 46% (w/v) DABCO PU-PEG and the 23% (w/v) DBTDL hydrogels' (p-value<0.01), whilst a highly significant difference was found between the 46% PU-PEG and the remaining hydrogel formulations: 23% (w/v) DABCO PU-PEG, 18% (w/v) DABCO PU-PEG, 15% (w/v) DABCO PU-PEG and 12% (w/v) DABCO PU-PEG (p-value<0.001). Although |G*| values were lower with diminished PU-PEG concentrations, no significant difference in these measurements was found between both 23% (w/v) DBTDL and DABCO PU-PEG, 18% (w/v) DABCO PU-PEG, 15% (w/v)

DABCO PU-PEG and 12% (w/v) DABCO PU-PEG hydrogels. The use of a different catalyst showed no significant impact in |G*| between the 23% (w/v) PU-PEG hydrogels.

Overall, the 46% (w/v) DABCO PU-PEG hydrogel displayed a higher resistance to forces in comparison to other hydrogel formulations.

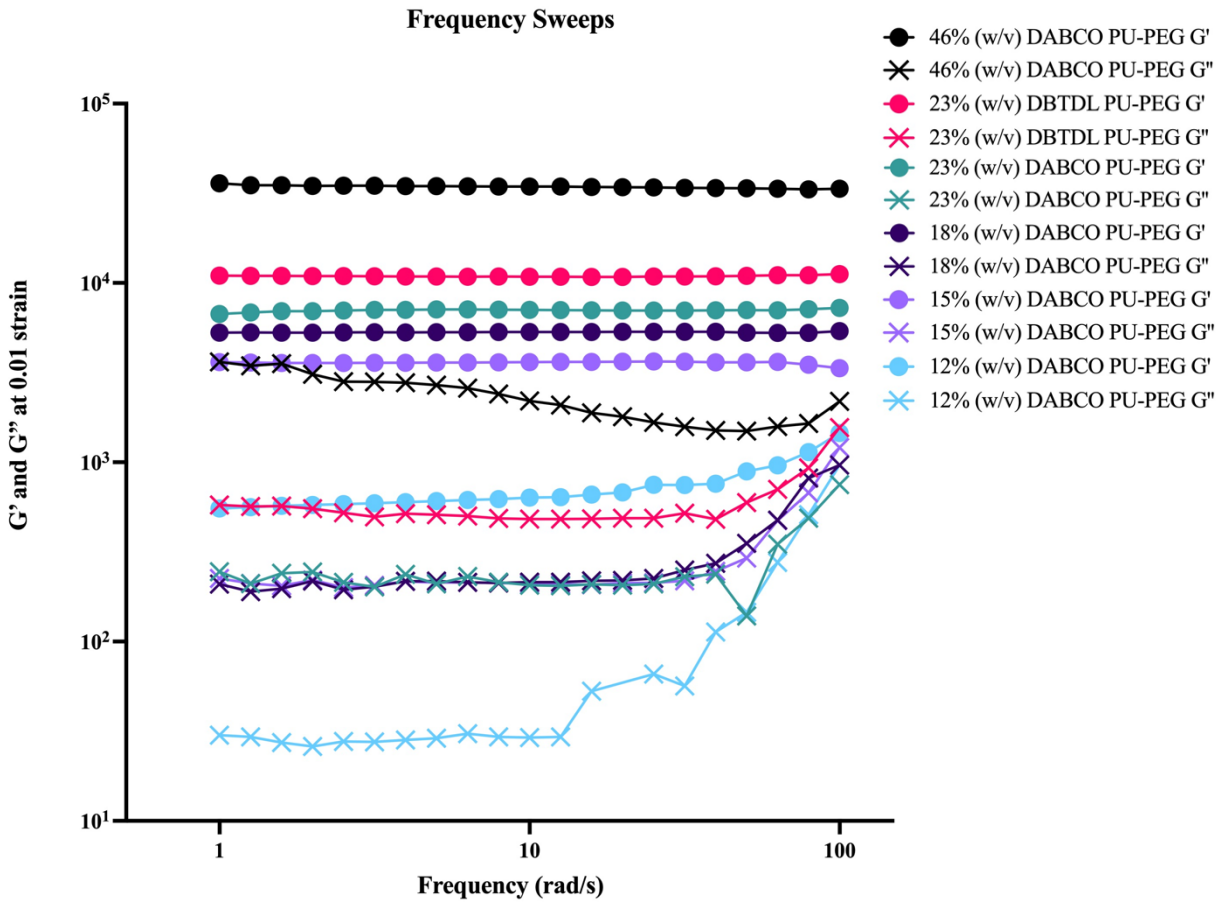

Figure 3.1 - PU-PEG hydrogel mechanical properties. Rheological profile of 46% (w/v) DABCO PU-PEG, 23% (w/v) DABCO PU-PEG, 23% (w/v) DBTDL PU-PEG, 18% (w/v) DABCO PU-PEG, 15% (w/v) DABCO PU-PEG and 12% (w/v) DABCO PU-PEG hydrogels at 22,5ºC. One representative frequency sweep of each gel formulation represented with storage modulus (G', solid components) and loss modulus (G'', liquid components) measured at a fixed strain of 0,01 (1%) and increasing frequency from 1 to 100 rad/s.

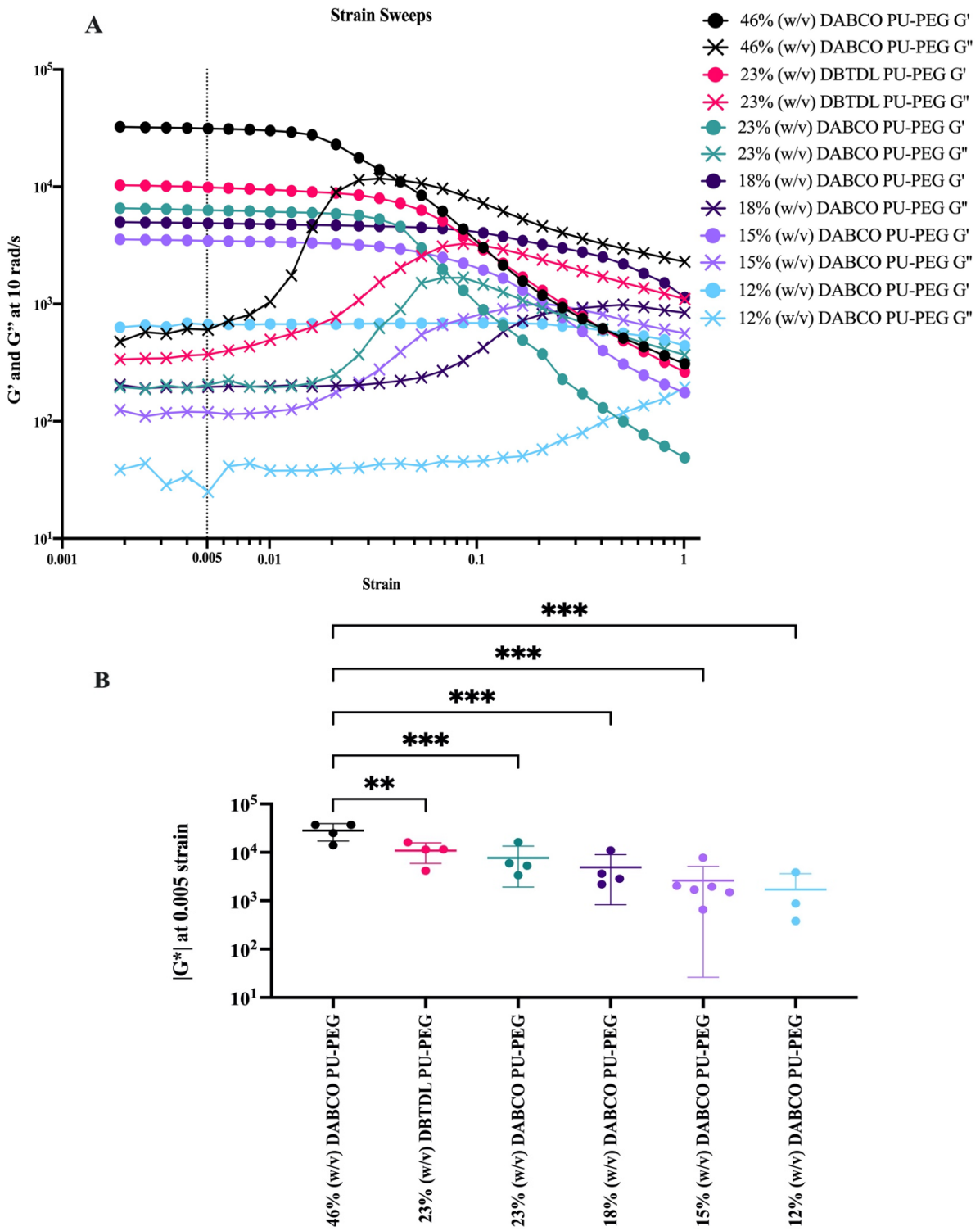

Figure 3.2 - PU-PEG hydrogels strain profile. Rheological profile of 46% (w/v) DABCO PU-PEG, 23% (w/v) DABCO PU-PEG, 23% (w/v) DBTDL PU-PEG, 18% (w/v) DABCO PU-PEG, 15% (w/v) DABCO PU-PEG and 12% (w/v) DABCO PU-PEG hydrogels at 22,5ºC. (A) One representative strain sweep with both storage modulus (G', solid components) and loss modulus (G'', liquid components) from each gel formulation at a fixed frequency of 10 rad/s and strain between 0.001 and 0.1. (B) Complex shear modulus (|G*|) at a strain value of 0.005. Results analyzed with one-way ANOVA and a Tuckey's test, n=3-6, *p*-value<0.05, Significance: ** if *p*<0.01; *** if *p* <0.001.

3.2. **Degradation and Swelling Studies**

A swelling and degradation study was performed to determine if the swelling ratio would differ between the hydrogel dilutions as well as if significant degradation occurred.

The swelling ratio of the hydrogels was affected by the concentration of PU-PEG (Figure 3.3), with lower swelling ratios associated with the more concentrated hydrogels. The swelling ratio of 46% (w/v) DABCO PU-PEG was 15.30 ± 2.65, whilst for 23% (w/v) DBTDL PU-PEG was 23.65 ± 7.392, for 23% (w/v) DABCO PU-PEG was 30.88 ± 6.274, for 18% (w/v) DABCO PU-PEG, was 31.59 ± 7.047, for 15% (w/v) DABCO PU-PEG was 37.22 ± 3.917 and for 12% (w/v) DABCO PU-PEG was 52.33 ± 5.462. Between the swelling ratio values of both 46% (w/v) DABCO PU-PEG and 18% (w/v) DABCO PU-PEG hydrogels there was a significant difference (p-value<0.05). A very significant difference was found between 46% (w/v) DABCO PU-PEG and 15% (w/v) DABCO PU-PEG, 23% (w/v) DABCO PU-PEG and 12% (w/v) DABCO PU-PEG, and 18% (w/v) DABCO PU-PEG and 12% (w/v) DABCO PU-PEG (p-value<0.01), whereas a highly significant difference was present between 46% (w/v) DABCO PU-PEG and 12% (w/v) DABCO PU-PEG as well as 23% (w/v) DBTDL PU-PEG and 15% (w/v) DABCO PU-PEG (p-value<0.001). No significant difference was found in the swelling ratio by using a different catalyst in the 23% (w/v) DBTDL and DABCO PU-PEG hydrogel samples.

Hydrogels' swelling ratios inversely correlate to their resistance to forces (Figure 3.4). At a 0.005 strain, hydrogels with lower swelling ratio, such as 46% (w/v) DABCO PU-PEG hydrogel, presented an increased capacity to resist deformation, with higher |G*|.

For all hydrogel formulations, no significant mass loss was present through the time course of the degradation assay (Figure 3.5). Freeze dried samples of both 46% (w/v) DABCO PU-PEG and 23% (w/v) DBTDL PU-PEG (Figure 3.5A - B), exhibited a folded shape and a darker color, and were also harder to the touch, whilst the 23% (w/v) DABCO PU-PEG, 18% (w/v) DABCO PU-PEG, 15% (w/v) DABCO PU-PEG and 12% (w/v) DABCO PU-PEG samples (Figure 3.7C - F) had a shape more closely resembling a disc and were whiter, and more sponge-like.

Hydrogel degradation of each sample at day 0 and at the end of the 35 days was, of -0.1643 ± 0.2503 % and -2.871 ± 1.978 % for 46% (w/v) DABCO PU-PEG, -1.324 ± 1.068 % and -4.237 ± 6.372 % for 23% (w/v) DBTDL PU-PEG, -2.030 ± 3.617 % and -2.601 ± 8.478 % for 23% (w/v) DABCO PU-PEG, -0.9123 ± 0.7280 % and 3.924 ± 1.923 % for 18% (w/v) DABCO PU-PEG, -0.8790 ± 0.5940 % and 0.3507 ± 5.449 % for 15% (w/v) DABCO PU-PEG and -3.251 ± 1.954 % and -12.07 ± 15.30 % for 12% (w/v) DABCO PU-PEG, respectively.

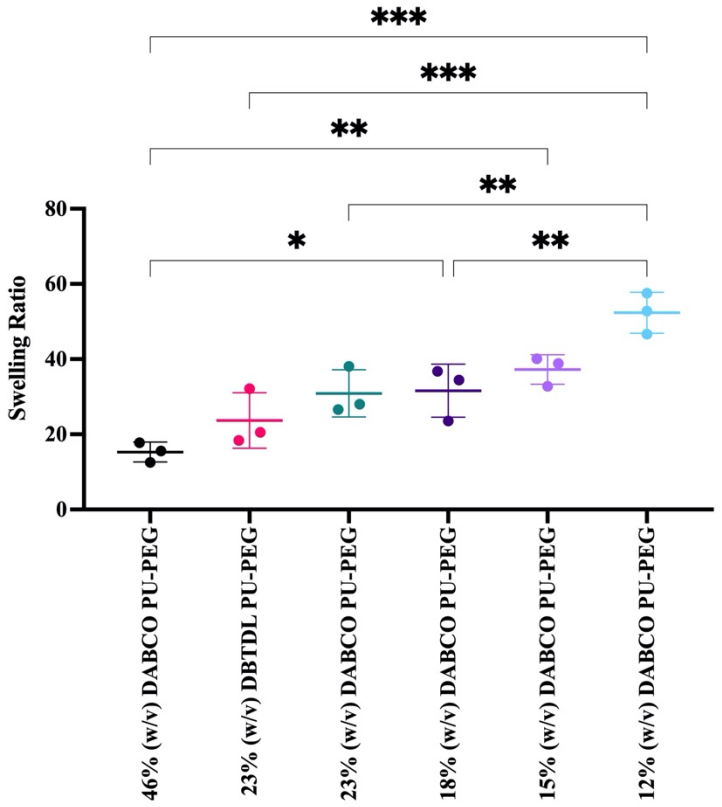

Figure 3.3 - PU-PEG hydrogels swelling behavior. Overall swelling ratios of 46% (w/v) DABCO PU-PEG, 23% (w/v) DABCO PU-PEG, 23% (w/v) DBTDL PU-PEG, 18% (w/v) DABCO PU-PEG, 15% (w/v) DABCO PU-PEG and 12% (w/v) DABCO PU-PEG hydrogels. Results analyzed with one-way ANOVA and a Tuckey's test, n=3, *p*-value < 0.05, Significance: * if $p < 0.05$; ** if $p < 0.01$; *** if $p < 0.001$.

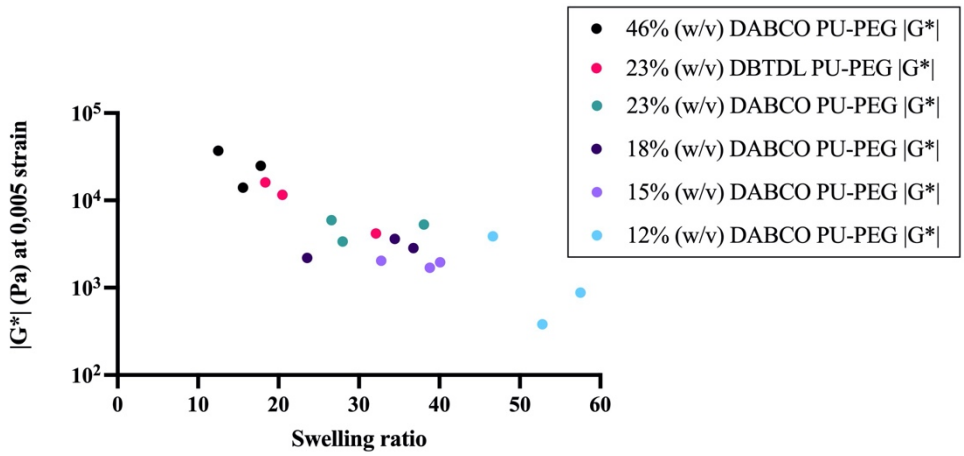

Figure 3.4 - Relation between PU-PEG hydrogels swelling behavior and corresponding rheological properties. Complex shear modulus (G*) at a strain value of 0.005 and a fixed frequency of 10 rad/s for 46% (w/v) DABCO PU-PEG, 23% (w/v) DABCO PU-PEG, 23% (w/v) DBTDL PU-PEG, 18% (w/v) DABCO PU-PEG, 15% (w/v) DABCO PU-PEG and 12% (w/v) DABCO PU-PEG hydrogels.

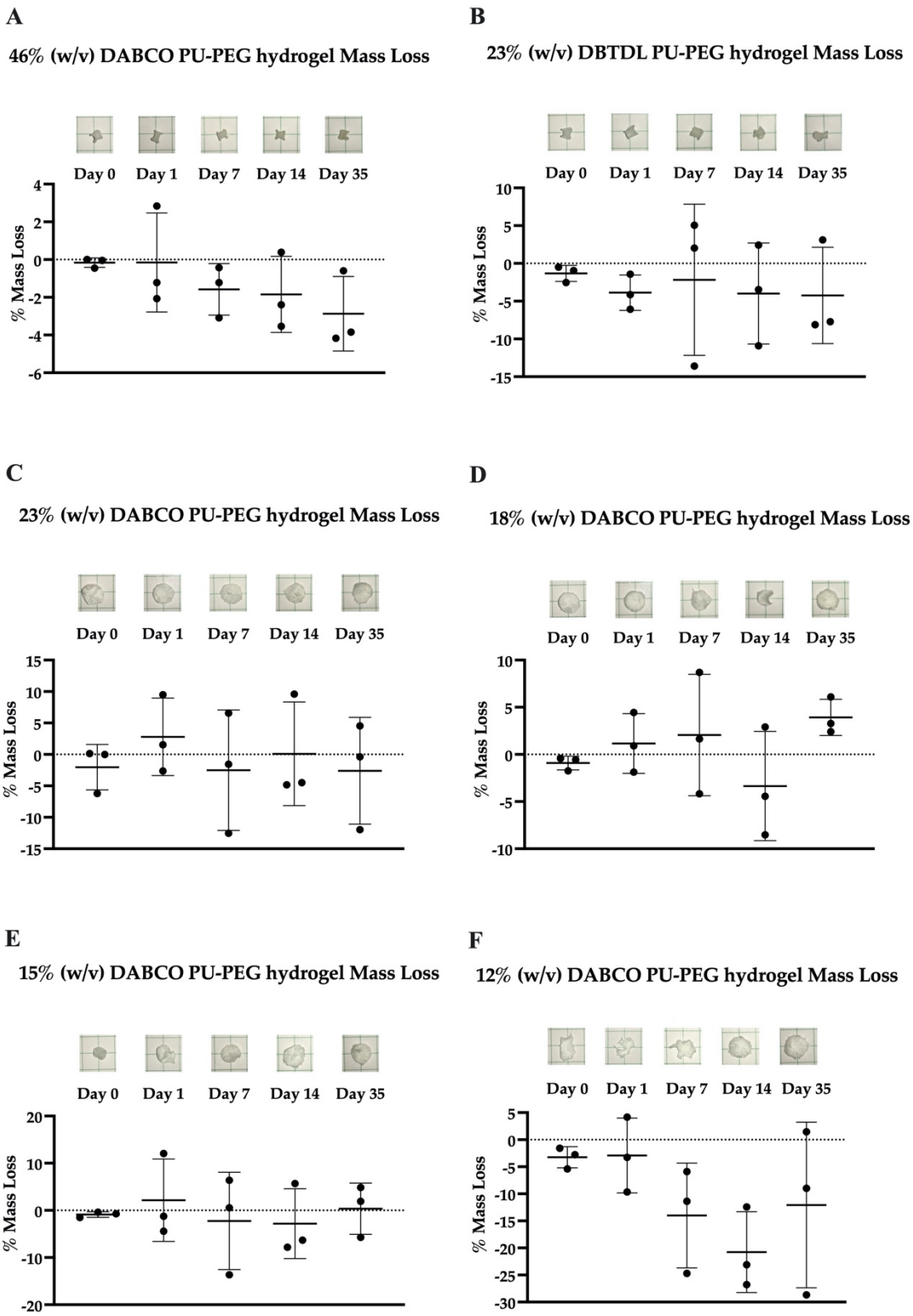

Figure 3.5 - PU-PEG hydrogels mass loss. Degradation of each hydrogel was measured over 35 days and the percentage of mass loss was determined. (A) 46% (w/v) DABCO PU-PEG hydrogels, (B) 23% (w/v) DBTDL PU-PEG hydrogels, (C) 23% (w/v) DABCO PU-PEG hydrogels, (D) 12% (w/v) DABCO PU-PEG hydrogels, (E) 15% (w/v) DABCO PU-PEG hydrogels and (F) 18% (w/v) DABCO PU-PEG hydrogels. Results analyzed with one-way ANOVA and a Tuckey's test, n=3, *p*-value >0.05.

3.3. Cytotoxicity evaluation

As a way to obtain cell metabolic activity, cell counting kit-8 (CKK8) was added to each extracted medium condition. This reagent is a salt that is reduced by dehydrogenases in cells to a colored product (formazan) that is soluble in the medium giving it an orange color, and that can be measured by absorbance reading at 450 nm. The amount of formazan produced by dehydrogenase activity in cells is directly proportional to the number of living cells.

In all assays polyethylene tubing was used as the negative control (NC) and citric acid as the positive control (PC). Both medium and no cells conditions represent internal controls for the assay, with the first one being used as a comparison with the polyethylene tubing condition to evaluate assay and cell conditions, whilst the second, wells with no cells and only complete media, was used to obtain the background signal of the assay in the instance that no cells were present. Measurements of the pH of the extracted media conditions were also made at RT for each assay.

To assess if lower hydrogel cytotoxicity would occur by using DABCO catalyst instead of DBTDL, due to the possibility of tin being retained in the hydrogel network depending on its casting condition, a cytotoxicity assay was carried out on both vial and flat samples from the 23% (w/v) DABCO PU-PEG and 23% (w/v) DBTDL PU-PEG hydrogels.

After a 24 h treatment of cells with extracted media, followed by three more hours of incubation with CCK8 reagent the cells metabolic activity was measured (Figure 3.6A). L929 fibroblast cells in polyethylene tubing (NC) extracted medium, and in both 23% (w/v) DABCO PU-PEG samples (Vial and Flat) had a similar cell metabolic activity, showing no toxicity. The same was observed with the 23% (w/v) DBTDL PU-PEG Flat sample. On the contrary, the 23% (w/v) DBTDL PU-PEG Vial sample showed a highly significant toxicity *(p*-value<0.001), similar to both citric acid (PC) and no cells, when compared to the polyethylene tubing. A higher variability was observed in the DBTDL vial samples when compared with the other samples.

At 72 h (Figure 3.6B), a similar trend was observed as with 24 h data. All analyzed data was normalized to polyethylene tubing and the background signal for the assay was removed, thus, cell metabolic activity in both polyethylene tubing and no cells was of 100.0 ± 0.000 %, and 0.000 ± 0.000 %, respectively. In citric acid condition, the cell metabolic activity at 24 h was of 1.518 ± 1.057 % and at 72 h was of 0.7477 ± 0.3910 %. For the remaining conditions, the metabolic activity observed at 24 h and 72 h, respectively, was of 91.53 ± 3.803 % and 96.33 ± 4.678 % in medium, 95.39 ± 3.096 % and 98.18 ± 2.676 % in 23% (w/v) DABCO PU-PEG Flat, 92.49 ± 2.384 % and 95.16 ± 5.326 % in 23% (w/v) DABCO PU-PEG Vial, 92.26 ± 11.53 % and 98.40 ± 5.475 % in 23% (w/v) DBTDL PU-PEG Flat and 28.18 ± 41.36 % and 32.29 ± 55.02 % in 23% (w/v) DBTDL PU-PEG Vial hydrogel samples.

The pH of the extracted media was measured (Figure 3.6C) from the conditions of both casts synthesized with either DABCO (8.733 ± 0.4619 vial, 8.100 ± 0.1000 flat) or DBTDL (9.000 ± 0.000 vial, 9.000 ± 0.000 flat) catalyst, where the extracted medium had a pH similar to polyethylene tubing

and medium of 9.000 ± 0.000 and 8.000 ± 0.000, respectively, contrasting with the acidic environment observed in the citric acid (3.067 ± 0.1155) condition.

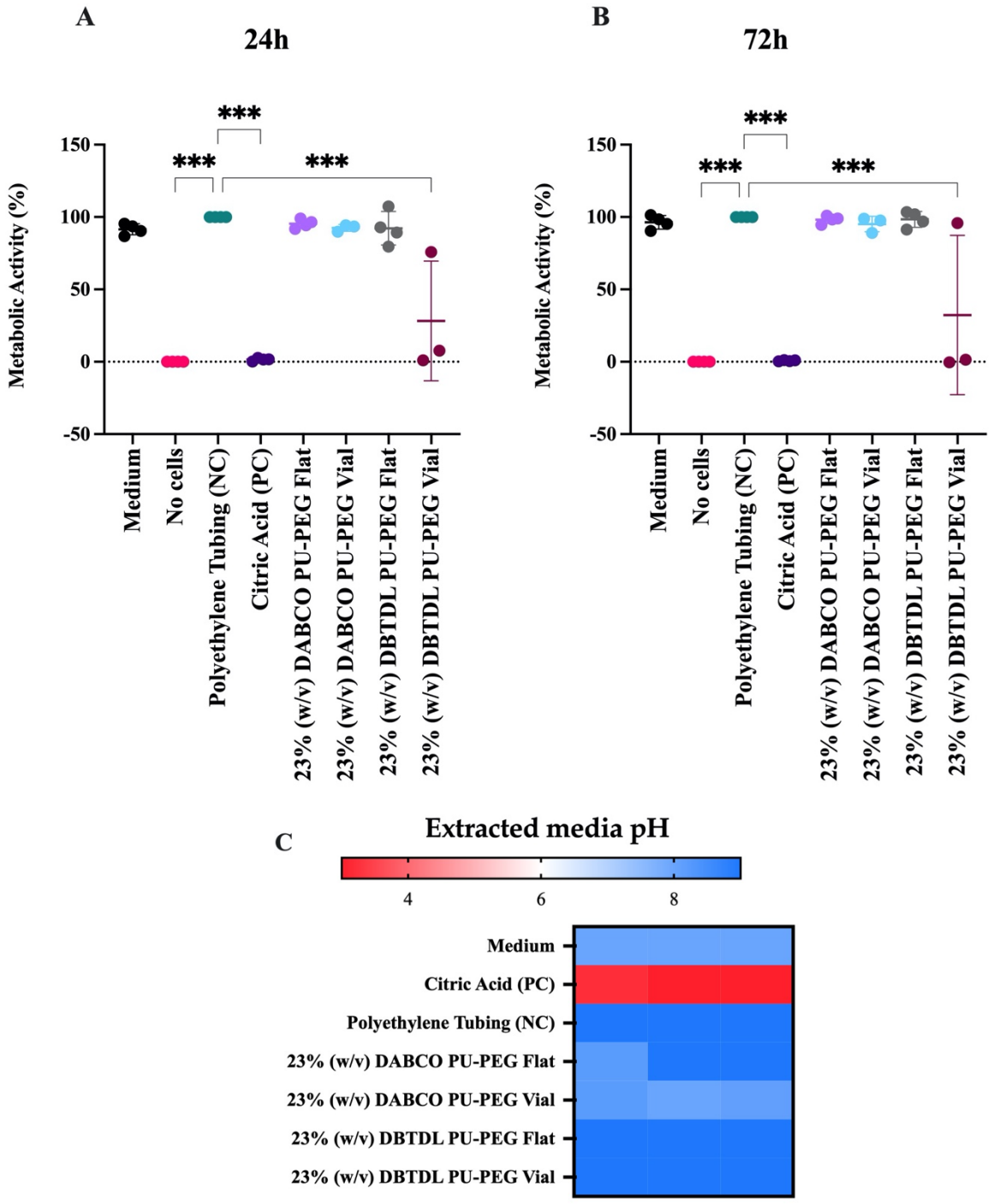

Figure 3.6 - Hydrogel cytotoxicity: Impact of casting form and catalyst and extracted media pH. Polyethylene tubing is the negative control (NC) and citric acid is the positive control (PC). Both medium and no cells conditions represent internal controls for the assay. Metabolic activity of L929 cell line measured with CCK8 after exposure to extracted media from 23% (w/v) DABCO PU-PEG Vial and Flat, and 23% (w/v) DBTDL PU-PEG Vial and Flat hydrogels after 24 h (A) and 72 h (B) of incubation at 37°C with 5% of CO_2. (C) pH measurements at RT of extracted medium. Cytotoxicity results analyzed with one-way ANOVA and a Tuckey's test, n=3-4, *p*-value<0.05, Significance: *** if p <0.001.

The tin (Sn118) content present in the synthesized samples was quantified by Inductively Coupled Plasma – Mass Spectrometry (ICP – MS), (results courtesy of Derrick Roberts) and can be found in figure 3.7. In the 23% (w/v) DBTDL PU-PEG Vial samples, the tin concentration present was of 1918 ± 1568 ppm, higher than the remaining samples. In the 23% (w/v) DBTDL PU-PEG Flat sample the tin concentration was 24.70 ± 16.94 ppm, and although lower than the 23% (w/v) DBTDL PU-PEG Vial, it was still higher than both 23% (w/v) DABCO PU-PEG Flat, 2.082 ± 2.463 ppm, and Vial, 1.633 ± 1.019 ppm samples, with no significant difference being present.

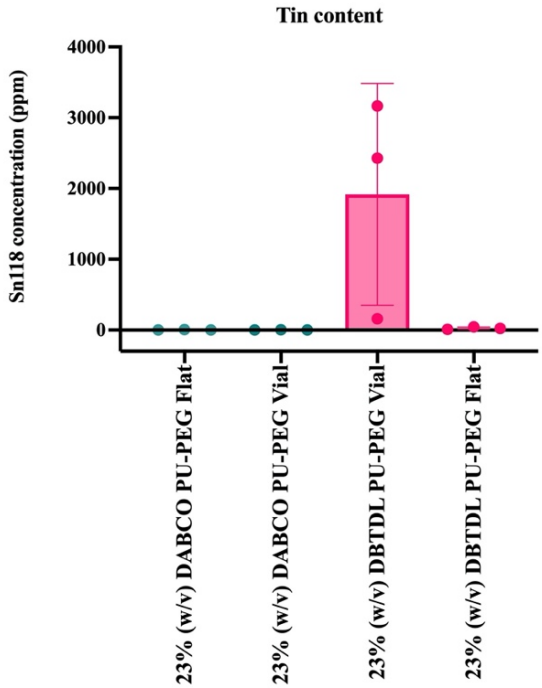

Figure 3.7 - Inductively Coupled Plasma – Mass Spectrometry (ICP – MS), (results by Derrick Roberts). Tin content (ppm) on both Vial and Flat casting forms of the 23% (w/v) DABCO PU-PEG and 23% (w/v) DBTDL PU-PEG hydrogels. Results analyzed with one-way ANOVA and a Tuckey's test, n=3, *p*-value<0.05.

The possibility to use the hydrogels as implants, lead to the study of blue food coloring as a marking option for these gels, to make them easier to retrieve after *in vivo* implantation. The cytotoxicity of different concentrations of blue food coloring was first examined with the same cell line (L929).

Higher concentrations of blue food coloring affected cell viability. At both 24 h (Figure 3.8A) and 72 h (Figure 3.8B) there was a significant difference (*p*-value<0.001) in toxicity in cells exposed to the two highest concentrations of blue food coloring used (0.77% (w/v) and 0.385% (w/v)), similar to the citric acid and no cells, when compared to the polyethylene tubing. On the contrary, no significant difference in cell survival was found between polyethylene tubing sample and the two lowest concentrations of blue food coloring (0.1295% (w/v) and 0.077% (w/v)) as well as in medium.

Metabolic activity corresponding to polyethylene tubing and no cells were set to 100.0 ± 0.000 % and 0.000 ±0.000 % at both time points. For medium, 0.1925% (w/v) blue food coloring and 0.077%

(w/v) Blue Food Coloring, cell metabolic activity at 24 h and 72 h were consistent between the two time-points with 107.3 ± 33.02 % and 107.6 ± 10.52 %, 76.55 ± 26.56 % and 121.4 ± 27.10 % and 106.1 ± 10.33 % and 124.1 ± 9.545 %, respectively. A decreasing tendency in cell metabolic activity was found in citric acid from 1.516 ± 1.188 % to 0.6230 ± 0.3376 %, in 0.385% (w/v) blue food coloring from -0.1920 ± 0.7734 % to -0.2978 ± 0.1714 % and in 0.77% (w/v) blue food coloring from 2.050 ± 0.4950 % to 1.150 ± 0.07071 %.

From the pH measurements of the extracted medium (Figure 3.8C), the higher blue food coloring concentrations, 0.77% (w/v) and 0.385% (w/v), had an acidic pH of 4.200 ± 0.000 and 5.200 ± 0.08165, respectively, close to citric acid's (3.033 ± 0.05774). The lowest blue food coloring concentrations, 0.1925% (w/v) and 0.077% (w/v), had a higher pH of 6.875 ± 0.2630 and 7.550 ± 0,1915, closer to the slightly basic values of both medium (8.100 ± 0.2000) and polyethylene tubing (9.000 ± 0.000) extracted media. The acidic pH of the two lower blue food coloring concentrations is in line with the high toxicity present in the metabolic assay of both extracted medias.

Further testing of the cytotoxicity of the hydrogel together with the blue food coloring at 0.74% (w/v) using the L929 cell line was carried out. Extracted media from hydrogels embedded in blue food coloring showed no cytotoxicity towards the cells. After 24 h (Figure 3.9A) and 72 h (Figure 3.9B), the cell metabolic activity was measured and at both time points, no significant cell death (p-value<0.05) was present between polyethylene tubing condition, 100.0 ± 0.000 %, and both extracted media from the 46% (w/v) DABCO PU-PEG hydrogel and the 46% (w/v) DABCO PU-PEG hydrogel w/ blue food coloring conditions. Citric acid and no cells presented a highly significant difference (p-value<0.001) when compared to polyethylene tubing.

At 24 h cell metabolic activity in medium condition was 110.6 ± 6.287 %, in citric acid was 0.7359 ± 1.791 %, in 46% (w/v) DABCO PU-PEG hydrogel was 102.3 ± 14.83 % and 46% (w/v) DABCO PU-PEG hydrogel w/ blue food coloring was 71.77 ± 32.72 %. While at 72 h cell metabolic activity in medium was of 106.3 ± 16.52 %, in citric acid was 0.6625 ± 0.8980 %, in 46% (w/v) DABCO PU-PEG hydrogel was 94.46 ± 2.722 %, and in 46% (w/v) DABCO PU-PEG hydrogel w/ blue food coloring was of 92.57 ± 30.10 %.

Measurements of the pH from the extracted media (Figure 3.9C) showed the 46% (w/v) DABCO PU-PEG hydrogel and 46% (w/v) DABCO PU-PEG hydrogel w/ blue food coloring had a pH of 8.700 ± 0.5196 and 7.933 ± 0.05774, close to both medium (8.000 ± 0.000) and polyethylene tubing (9.000 ± 0.000), whilst citric acid pH was of 3.050 ± 0.07071.

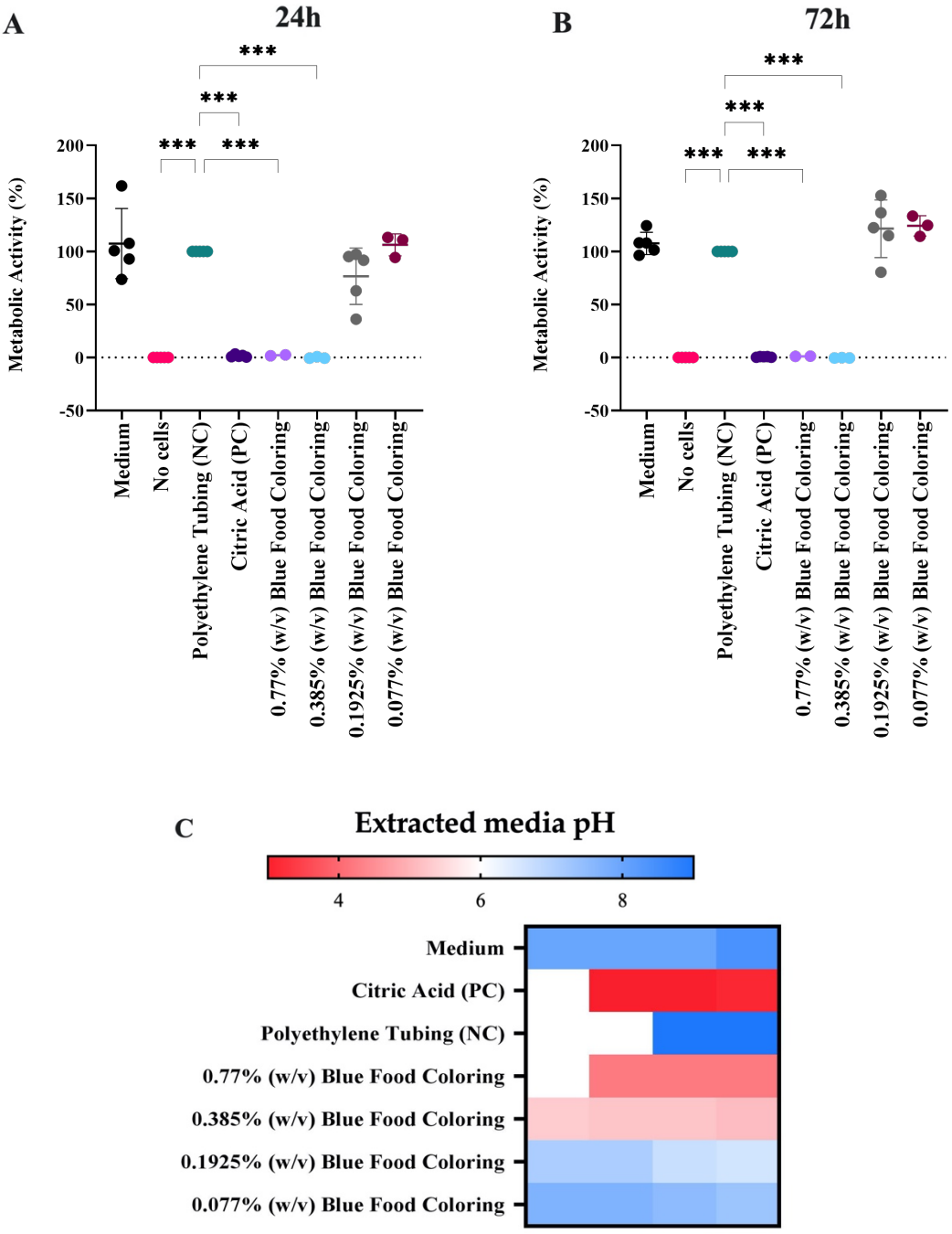

Figure 3.8 - Blue food coloring cytotoxicity and extracted media pH. Polyethylene tubing is the negative control (NC), and citric acid is the positive control (PC). Both medium and tissue culture plastic conditions represent internal controls for the assay. Metabolic activity of L929 cell line measured with CCK8 after incubation at 37°C with 5% of CO_2 in Blue food coloring dilutions %(w/v): 0.77%, 0.385%, 0.1925% and 0.077% for 24 h (A) and 72 h (B). (C) pH values of extracted media measured at RT Cytotoxicity results analyzed with one-way ANOVA and a Tuckey's test, n=3-5, *p*-value<0.05, Significance: *** if p <0.001.

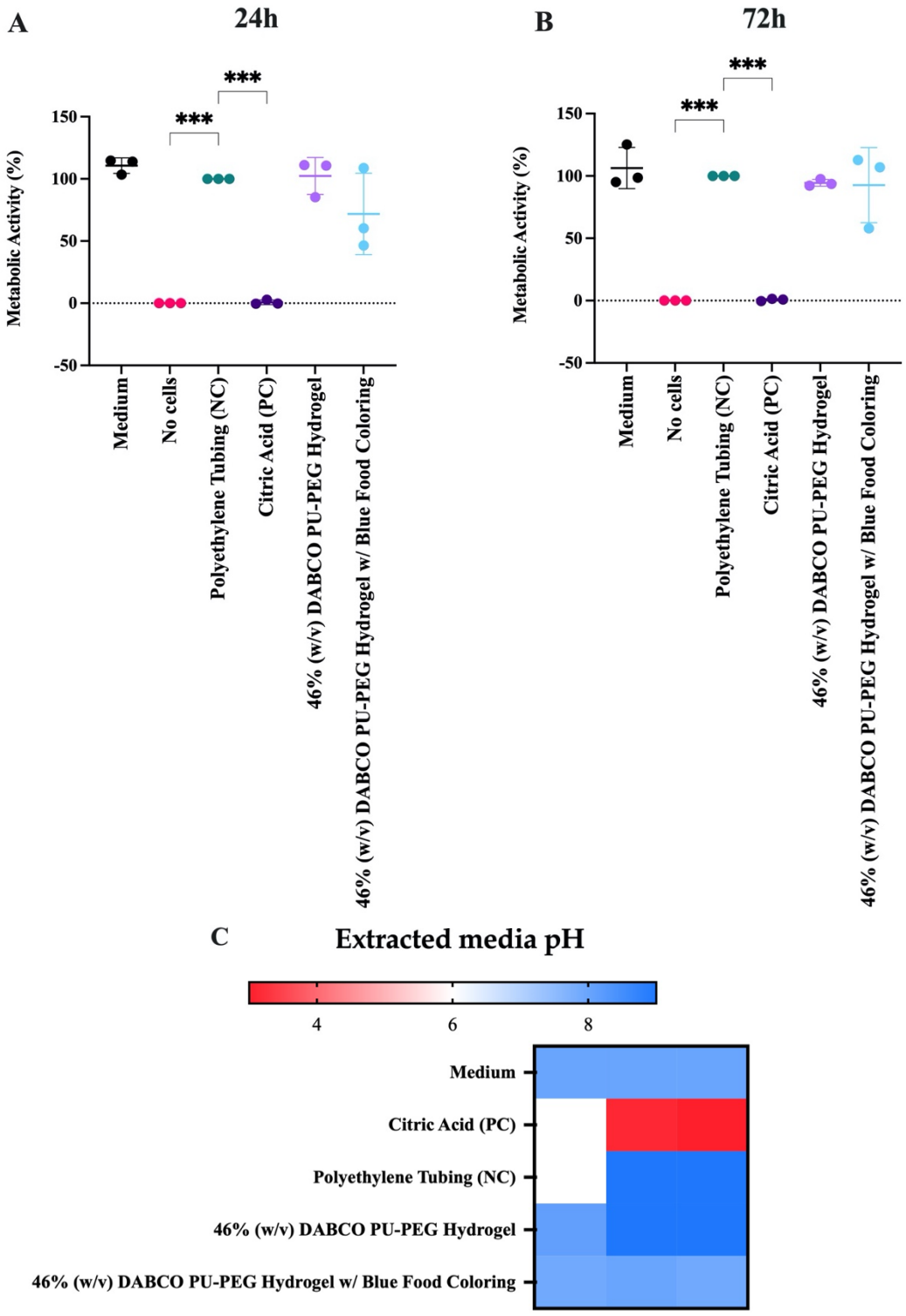

Figure 3.9 - Hydrogels immersed in blue food coloring toxicity and extracted media pH. Polyethylene tubing is the negative control (NC), and citric acid is the positive control (PC). Medium and tissue culture plastic conditions represent internal controls for the assay. Metabolic activity L929 cell line measured with CCK8 after incubation at 37°C with 5% of CO_2 in extracted medias from 46% (w/v) DABCO PU-PEG hydrogel only and embedded in 0.74% (w/v) of blue food coloring after 24h (A) and 72h (B). (C) Extracted Media pH Measurements made at RT. Cytotoxicity results analyzed with one-way ANOVA and a Tuckey's test, n=3-5, *p*-value<0.05, Significance: *** if $p<0.001$.

3.4. **Protein Adsorption**

To evaluate the nonfouling properties of the PU-PEG hydrogels, protein adsorption of the hydrogel formulations in comparison to PDMS (50:1) gel was studied using Bicinchoninic Acid (BCA), a molecule that forms a complex with a cuprous cation (Cu^{+1}) originated from the reduction of Cu^{+2} to Cu^{+1} by proteins in alkaline environments. This complex has a purple color, and its absorbance can be measured at 562 nm. Calibration curves were made for both bovine serum albumin (Figure 3.10A) and bovine plasma fibrinogen (Figure 3.10B) to determine the concentration of each adsorbed protein.

For each PU-PEG hydrogel and PDMS gel, the concentration of adsorbed protein measured is present in figure 3.11. The concentration of adsorbed albumin (Figure 3.11A) showed a tendency to increase from the 46% (w/v) DABCO PU-PEG hydrogels having an average concentration of the adsorbed protein of 4.830 ± 6.062 μg/mL, followed by 23% (w/v) DBTDL PU-PEG with 56.52 ± 71.93 μg/mL, 23% (w/v) DABCO PU-PEG with 64.11 ± 36.64 μg/mL, 18% (w/v) DABCO PU-PEG with 104.4 ± 30.54 μg/mL, 15% (w/v) DABCO PU-PEG with 184.4 ± 75.22 μg/mL and 12% (w/v) DABCO PU-PEG with 211.9 ± 199.7 μg/mL of albumin. A significant statistical difference (p-value<0.05) was found between the concentration of albumin adsorbed by 12% (w/v) DABCO PU-PEG hydrogel and the PDMS gel, where an immensely low concentration of albumin was present at -0.335 ± 17.68 μg/mL.

In comparing the various PU-PEG hydrogels and the concentration of adsorbed fibrinogen (Figure 3.11B), an increased amount of fibrinogen in 12% (w/v) DABCO PU-PEG hydrogel of 148.1 ± 138.8 μg/mL, was found to be significant (p-value<0.05) when compared to that on the PDMS gel controls with 12.83 ± 12.92 μg/mL of fibrinogen. The adsorbed fibrinogen concentration for the remaining samples was of 10.22 ± 16.45 μg/mL for 46% (w/v) DABCO PU-PEG, 28.70 ± 12.99 μg/mL for 23% (w/v) DABCO PU-PEG hydrogel, 14.76 ± 0.4799 μg/mL for 23% (w/v) DBTDL PU-PEG, 17.01 ± 18.51 μg/mL for 18% (w/v) DABCO PU-PEG and 21.76 ± 16.40 μg/mL for 15% (w/v) DABCO PU-PEG hydrogel.

Albumin adsorption showed a tendency to be higher than fibrinogen adsorption. In both cases, the 12% (w/v) DABCO PU-PEG hydrogels showed the highest amount of protein adsorption and when compared to PDMS, these differences were statistically significant. The usage of a different catalyst does not show statistical differences in protein adsorption.

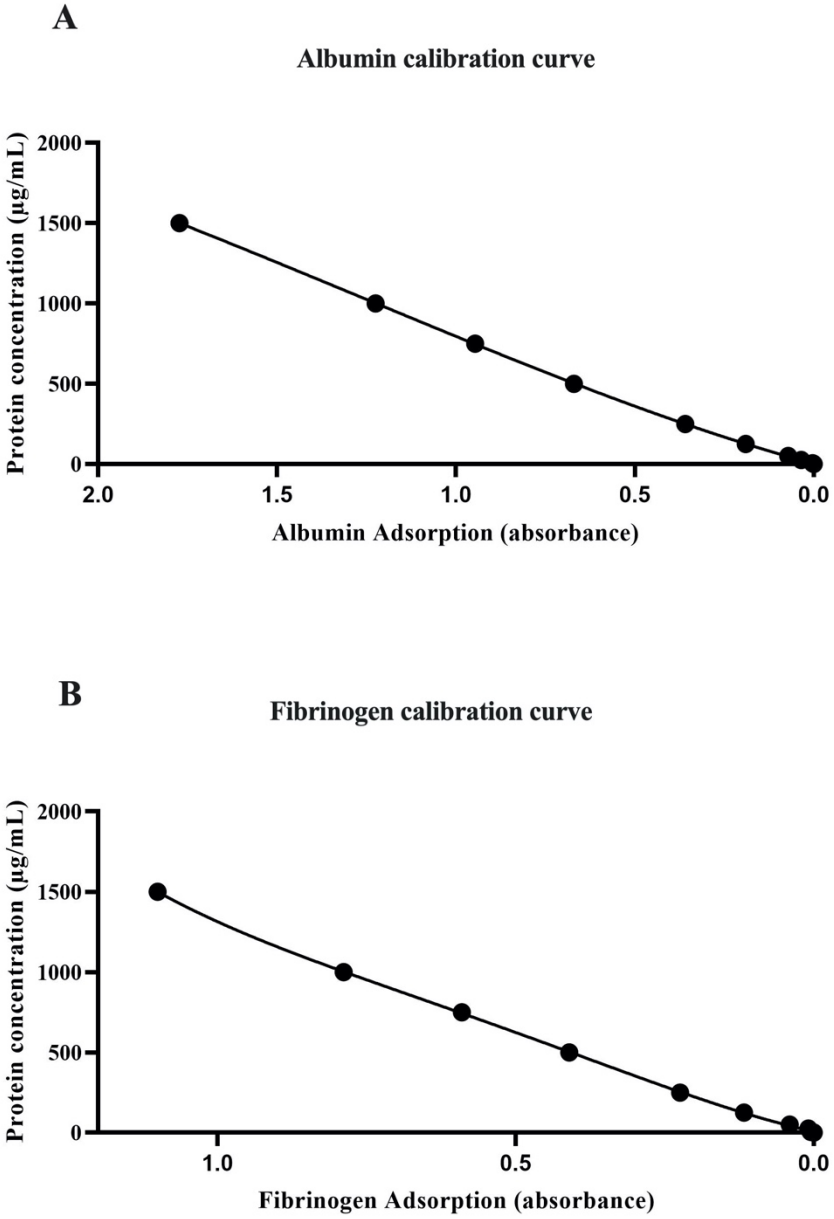

Figure 3.10 - Calibration curves from protein adsorption. Bicinchoninic acid (BCA) complexation to Cu^{+1} was measured at 562 nm with known bovine serum albumin and bovine plasma fibrinogen concentrations. Fourth order polynomial calibrations curves were determined for (A) Albumin ($R^2 = 1$; $y = 2{,}1495x^4 - 76{,}221x^3 + 265{,}79x^2 + 601{,}05x + 2{,}7614$) and (B) Fibrinogen ($R^2 = 0{,}9999$; $y = 1182{,}6x^4 - 2491{,}6x^3 + 1813{,}2x^2 + 801{,}65x + 8{,}1345$). Results obtained from 3 experimental repeats with 3 replicates for each concentration, and equations were obtained with Microsoft Excel.

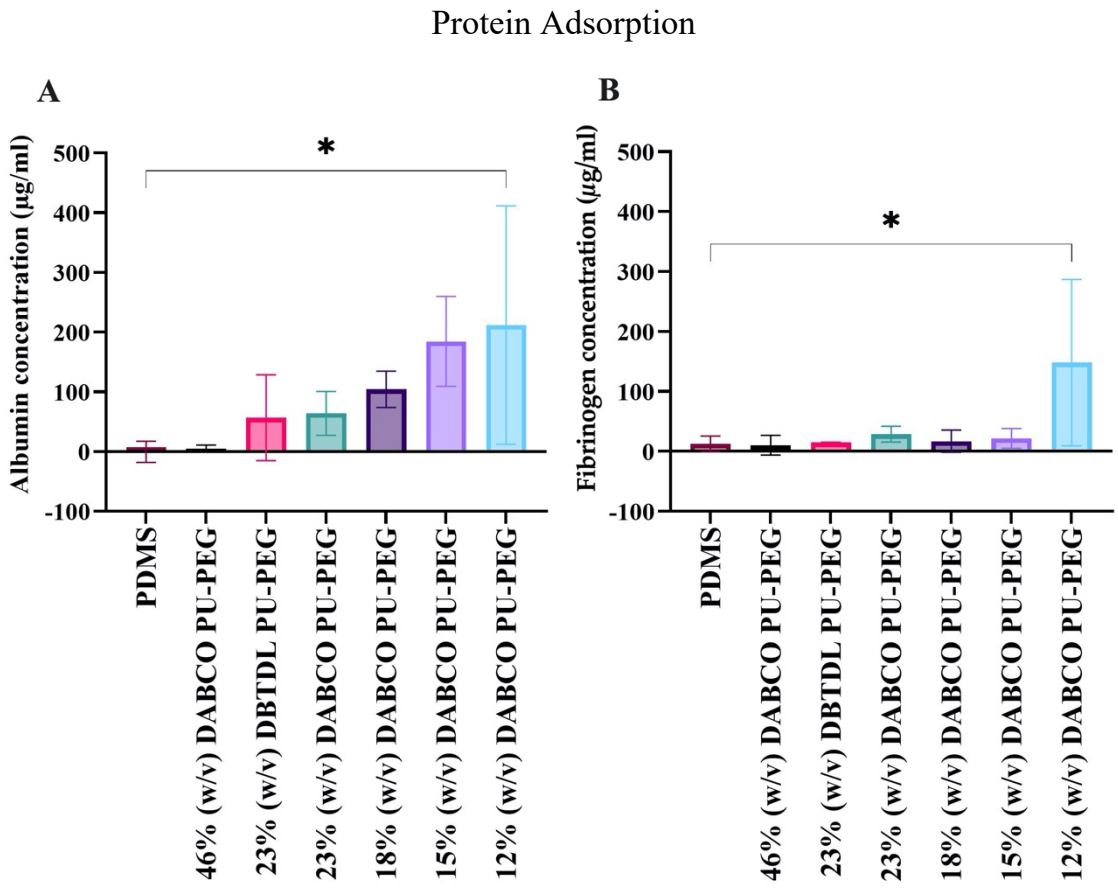

Figure 3.11 - Concentration of adsorbed proteins. PDMS (50:1) and 46% (w/v) DABCO PU-PEG, 23% (w/v) DABCO PU-PEG, 23% (w/v) DBTDL PU-PEG, 18% (w/v) DABCO PU-PEG, 15% (w/v) DABCO PU-PEG and 12% (w/v) DABCO PU-PEG hydrogel samples protein concentration was quantified for (A) Albumin and (B) Fibrinogen. Results analyzed with one-way ANOVA and a Tuckey's test, n=3-4, *p-value*<0.05, Significance: *if $p< 0.05$.

3.5. Cell adhesion

To further investigate the nonfouling potential of the synthesized PU-PEG hydrogels, a cell adhesion assay was conducted with the L929 fibroblasts.

The 23% (w/v) DABCO PU-PEG hydrogels were used in this to allow for a better comparison to PDMS since their mechanical stiffness is similar to PDMS at 50:1. The 46% (w/v) DABCO PU-PEG, 15% (w/v) DABCO PU-PEG and 12% (w/v) DABCO PU-PEG hydrogels were also selected as they represent the mechanical forces extremes obtained in the mechanical characterization for the hydrogel formulations synthesized, providing a broader spectrum of results. L929 cells were seeded on the PU-PEG hydrogels and PDMS gel surfaces and incubated for 24 h at 37ºC with 5% CO_2. Cell adhesion was assessed by staining with DAPI for nuclei marking (Figure 3.12).

PDMS

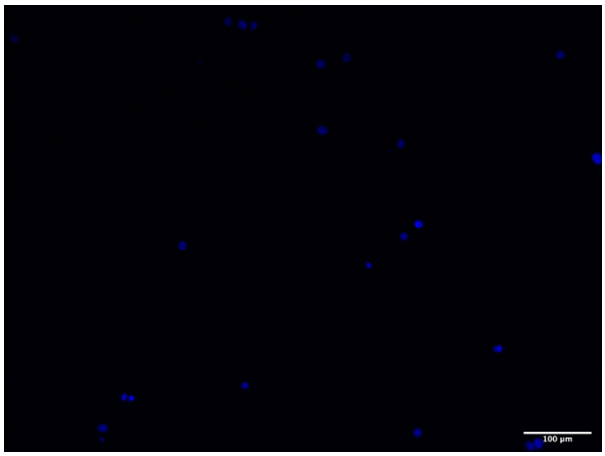

46% (w/v) DABCO PU-PEG

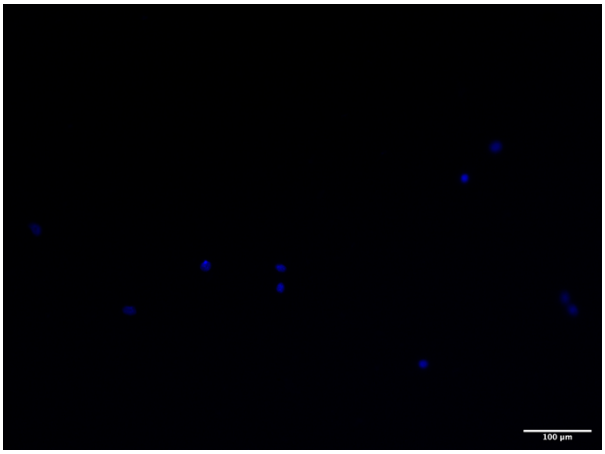

23% (w/v) DABCO PU-PEG

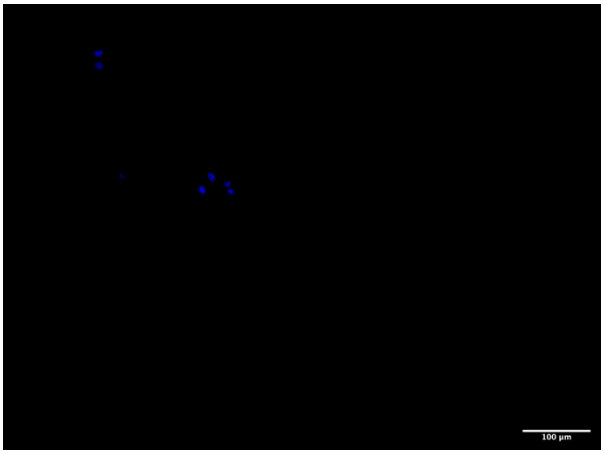

15% (w/v) DABCO PU-PEG

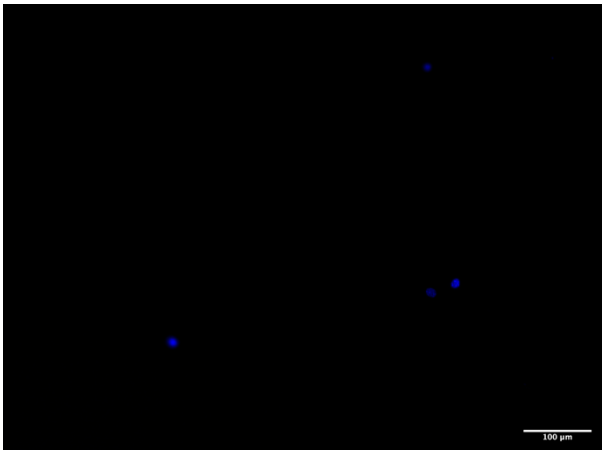

12% (w/v) DABCO PU-PEG

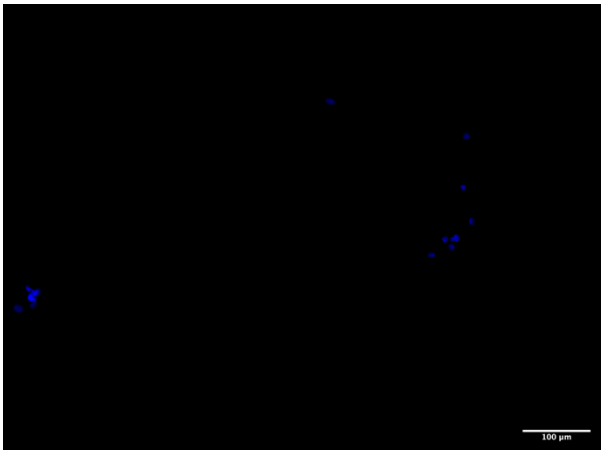

Figure 3.12 - Cellular adhesion. L929 cell line cultured on PDMS (50:1) and 46% (w/v) DABCO PU-PEG, 23% (w/v) DABCO PU-PEG, 15% (w/v) DABCO PU-PEG and 12% (w/v) DABCO PU-PEG samples for 24 h to evaluate nonfouling properties, followed by fixation and nuclear staining with DAPI for cell count. Images taken in Axio imager 2, scale bar at 100 µm.

Quantification of the cell number per area was determined for all conditions, by two different methods: directly counting all cells in the microscope upon observation and dividing by the entire surface area of the hydrogel (Microscope cell count, Figure 3.13A) or by counting afterwards from images obtained from the microscope with Fiji, determining the number of cells per image and dividing by the area of the counted squares (Fiji cell count, Figure 3.13B). Cell count from the microscope upon observation was not possible for PDMS samples as the cell density was very high.

Between the PU-PEG hydrogel samples, where the cells were counted directly in the microscope, no significant difference was shown (Figure 3.13A) with 3.057 ± 1.828 cells/mm^2 in the 46% (w/v) DABCO PU-PEG hydrogel, 2.704 ± 0.6758 cells/mm^2 in the 23% (w/v) DABCO PU-PEG hydrogel, 1.539 ± 0.9426 cells/mm^2 in the 15% (w/v) DABCO PU-PEG and 4.330 ± 2.883 cells/mm^2.

Regarding the samples were the cell count obtained from Fiji was divided by the area of the square counted (Figure 3.13B), the number of cells adhered was of 38.16 ± 21.89 cells/mm^2 in the PDMS samples, followed by both 46% (w/v) DABCO PU-PEG, with 13.37 ± 8.055 cells/mm^2, 12% (w/v) DABCO PU-PEG with 17.65 ± 7.370 cells/mm^2, 23% (w/v) DABCO PU-PEG with 9.899 ± 1.773 cells/mm^2 and 15% (w/v) DABCO PU-PEG with 5.944 ± 2.044 cells/mm^2. No statistical differences were found between the PDMS samples and the PU-PEG hydrogel formulations.

When possible, the methods used for cell count were compared using the obtained values for cell number per area, as shown in figure 3.13C-E. There was more variability within the Fiji cell count values when compared with the other method. Between the 46% (w/v) DABCO PU-PEG and 15% (w/v) DABCO PU-PEG hydrogels (Figure 3.13C and 3.13F) no significant statistical difference was found in cell number per area between Fiji cell count and the microscope count. However, for the 12% (w/v) DABCO PU-PEG and 23% (w/v) DABCO PU-PEG hydrogels (Figure 3.13D and 3.13E), a significant (p-value<0.05) and very significant difference (p-value<0.01), respectively, was displayed between Fiji cell count and microscope cell count methods.

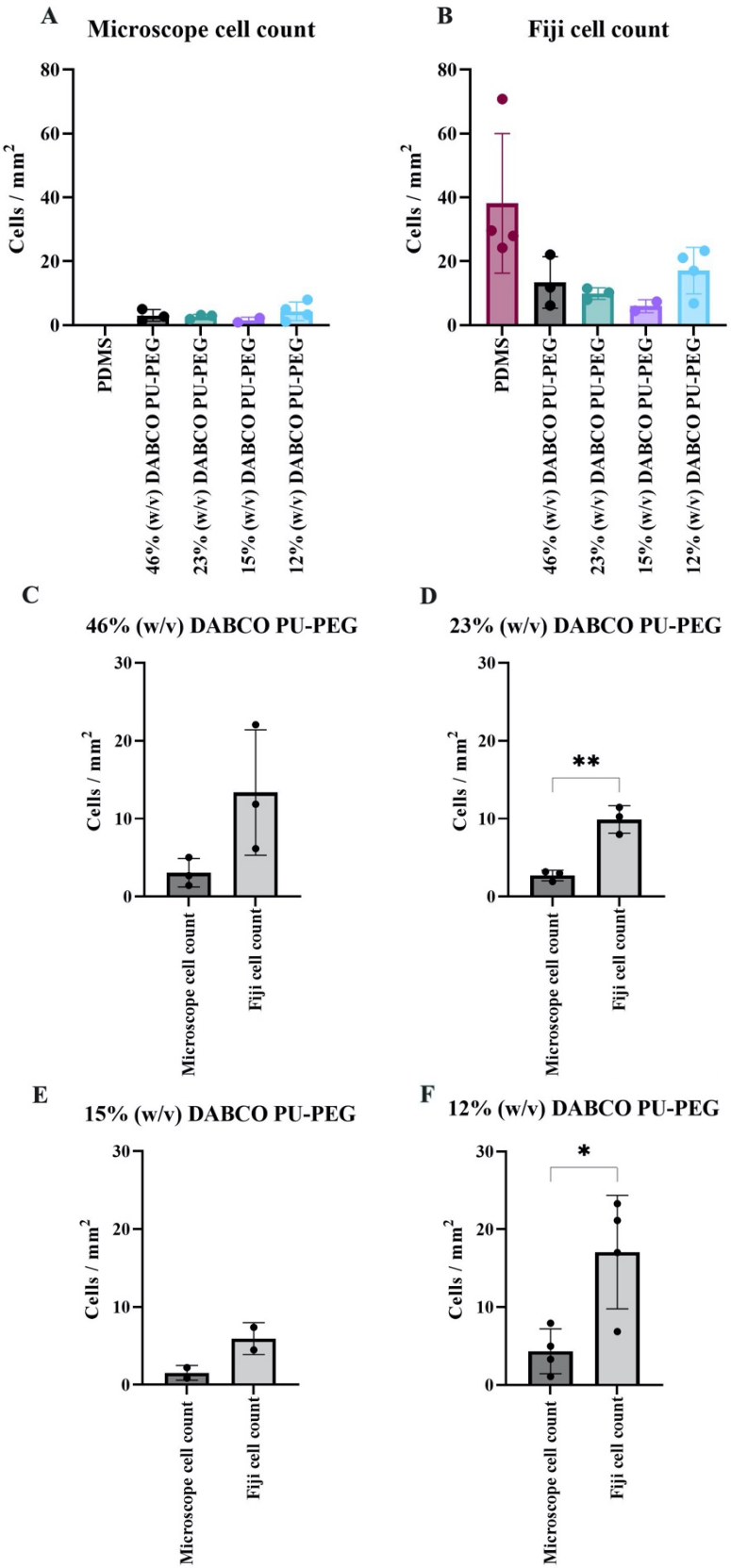

Figure 3.13 - Cell number per area. (A) Microscope cell count obtained by total cell number counted divided by the hydrogel surface area (PDMS cell count was not possible as the cell density was very high); (B) Fiji cell count from cell number in each image divided by the area of the counted square. Comparison between methods for each sample: (C) 46% (w/v) DABCO PU-PEG, (D) 23% (w/v) DABCO PU-PEG, (E) 15% (w/v) DABCO PU-PEG and (F) 12% (w/v) DABCO PU-PEG. Results analyzed with one-way ANOVA and a Tukey's test, n=2-4, p-value<0.05, Significance: * if $p< 0.05$; ** if $p <0.01$.

4. DISCUSSION

In this work, the studied PU-PEG hydrogels were shown to be biocompatible and their nonfouling potential was unveiled, presenting a promising candidate material for wound healing applications.

Compatibility and tolerance of the materials to the mechanical strains present in wound environments is a key feature in hydrogel characterization, as it could impact the hydrogels' interface with the surrounding tissue, and consequently affect its performance, as even low shear forces can impact the interface between the skin and a percutaneous implant, preventing its complete occlusion [48]. Frequency sweeps were performed within values that correspond to the usual daily activities, such as walking, jogging, and running (0.1 to 12 Hz) [48], with the hydrogels tolerating these frequencies well, maintaining their mechanical behavior (Figure 3.1). The hydrogels were solid and remained so over the course of the testing conducted as demonstrated by their G' > G''.

At a low magnitude strain of 0.005 the |G*| values for the hydrogels range from around 1,7 kPa to 28 kPa, displaying a wide range of mechanical properties, and that are in line with what has been studied for tissues with soft to intermediate softness in humans and model organisms [49,50]. Hydrogel PU-PEG content appeared to directly correlate to higher overall material strength (Figure 3.2B). Such was expected as it has been shown in PU-based hydrogels, synthesized with PEG, that increasing PEG content decreases the hydrogels' mechanical properties [34].

Assuming Poisson's ratio of 0.5 for hydrogels [50], the |G*| obtained in this experiment are also compatible with previous characterization studies of hydrogels for wound healing, with similar strength ranges. In a study on *in situ*-forming hydrogels as wound dressings for infected wound treatment in mice, the hydrogels strength was around 1 kPa to 6 kPa [51] and in the study of a diabetic foot wound dressing it was around 6 kPa [52].

Further characterization of the PU-PEG hydrogels displayed an inversely proportional relationship between the |G*| and the swelling ratio, which is in agreement with previous studies in Poly(ethylene glycol) – polyurethane hydrogels [33]. Additionally, a wide range of swelling ratios that showed a tendency to increase as PU-PEG concentration decreases from 46% (w/v) to the 12% (w/v) DABCO PU-PEG hydrogel (Figure 3.3), indicating that the studied hydrogel formulations can retain different levels of water content. This highlights an important characteristic that is ideal for wound dressings and

wounded areas, as high water content can keep the damaged areas moist and hydrated, when the hydrogel is in a swollen state, being capable of adsorbing wound exudates, when in a dried or semi-dried state, culminating in successful healing [28,53]. Depending on the needs of the wound and the extent of damage, different hydrogel formulations, with diverse swelling degrees, could be chosen to provide the ideal care [53]. Moreover, with no degradation reported in any hydrogel formulation, during the 35 days of the study (Figure 3.5), this biomaterial, could present a good option for wound healing and recovery, as the possibility of the PU-PEG hydrogels remaining in the wound environment could provide a cooling and soothing effect due to their water content and perhaps offer a barrier against infectious microorganisms [28,53]. Nonetheless, *in vivo* degradation was not studied in this work which could impact longer term applications in PEG-based hydrogels, as shown in previous works [26,54].

With biocompatibility studies of the PU-PEG hydrogels *in vitro*, it was clear that the substitution of the catalyst to DABCO from DBTDL provided a possible way to avoid the retention of the toxic tin component in the hydrogel meshes. As observed in the cytotoxicity results from the casting set-up and catalyst (Figure 3.6 A-B), the toxic effect was mainly present on the 23% (w/v) DBTDL PU-PEG Vial. This is likely due to tin, as seen in the ICP-MS data (Figure 3.7), a toxic element present in the DBTDL catalyst that remained trapped inside the hydrogel structure and was not washed out after full hydrogel crosslinking occurred, which made it an unviable cast as the tin concentration present in the samples was enough to cause a high cell death. Previous studies reported that when comparing DBTDL to DABCO, the DBTDL catalyst was capable of inhibiting cell growth to a greater extent in two different cell lines, mouse fibroblasts (Swiss 3T3) and Human endothelial cells (HEC), when the cells were directly in contact with different concentrations of the catalysts [55]. In this same study, the cytotoxicity of the DBTDL in a synthesized polymer of poly-urethane-amide demonstrated minimal fibroblast growth in medium extracted from the polymers [55], which is consistent with what was observed in this present work.

Within the 23% (w/v) DBTDL PU-PEG vial replicates, variations in tin concentrations were present coinciding with the experimental samples that exerted a less toxic effect. Although some traces of tin were found in the 23% (w/v) DBTDL PU-PEG flat (Figure 3.7) such quantity did not affect the cell living conditions. Similar results were found in the original work the synthesis was adapted from, where the hydrogel synthesized with the DBTDL catalyst appeared to promote cell survival [35]. Nonetheless, the substitution to the DABCO catalyst presents a solution to avoid the cytotoxic effect of DBTDL in both cast forms, promoting cell survival, cementing their potential as a biomaterial for tissue engineering and also wound healing [28].

To use PU-PEG hydrogels as possible subcutaneous implants, the option of marking them with blue food coloring for easier implant recovery was tested, based on previous *in vitro* and *in vivo* studies where no toxic effects were induced by this dye [56]. Initial toxicity of the blue food coloring was evaluated using four different concentrations, where the two highest blue food coloring concentrations (0.77% (w/v) and 0.385% (w/v)) presented a toxic effect towards the cells, in contrast with the two lowest

concentrations (0.1925% (w/v) and 0.077% (w/v)), that displayed no toxicity (Figure 3.8A-B). It should be noted that the assay in this work was performed in a static cell culture meaning that natural bioprocesses found in dynamic systems, for instance, dilution and perfusion of the food dye through the blood are not present, thus, the effect of the acidic pH from the extracted media of the two highest concentrations is more pronounced in this static condition (Figure 3.8C). Considering this, when selecting the food dye concentration for implant marking, only the two lowest blue food coloring concentrations should be accounted for, as even if the body can tolerate a larger range of pHs in comparison to a static cell culture condition, using a safe concentration in this last condition, would also be safe for *in vivo* application. If using the blue food coloring directly from its commercially available format, the stock solution (at 0.74% (w/v) of blue food coloring) should be diluted to 26% (v/v) or 10.4% (v/v) of blue food coloring, so that it would match either the 0.1925% (w/v) or the 0.077% (w/v) blue food coloring concentrations, as they seem to be non-toxic, and present a neutral pH.

Furthermore, the PU-PEG gels immersed in blue food coloring, by not displaying an impact on cell survival (Figure 3.9), showed that the amount of the food dye retained by the hydrogels when stained is not toxic to cells.

It is also worth noting that the pH of the extracted media in these cytotoxicity assays does not appear to have an impact on cell survival other than on the citric acid, which was excepted due to being the positive control, and on the previously mentioned both highest blue food coloring dilutions. Additionally, due to the pH measurements being made at RT after air exposure, where CO_2 levels are low, an increase in pH from the extracted media due to the presence of sodium bicarbonate could occur. This was observed in both medium and polyethylene tubing conditions where the pH values were slightly basic (Figure 3.6C, 3.8C and 3.9C).

PU-PEG hydrogel nonfouling properties were studied, and, although PEG is characterized as a nonfouling material, with low protein adsorption, due to its hydrophilic nature, non-specific adsorption of blood proteins has been observed in self-assembled monolayers with PEG-based surface coating [57], as well as on PEG-based hydrogels [58] and PEG grafting of phospholipid monolayers [59]. This was also observed in our results, as different levels of protein adsorption for the PU-PEG hydrogel formulations were displayed, with the highest concentration of adsorbed protein being from the 12% (w/v) DABCO PU-PEG hydrogel when compared to PDMS (Figure 3.11). This might be related to the hydrogels' water content, which also has a similar trend to the protein's adsorption (Figure 3.3) with higher swelling ratio on the least concentrated hydrogel (12% (w/v) DABCO PU-PEG). Higher water-content present in hydrogels could influence protein adsorption by facilitating protein diffusion into the hydrogel net in addition to surface only adsorption, when compared to PDMS [58]. Nonetheless, PU-PEG content does also seem to have a tendency to influence protein adsorption with the 46% (w/v) DABCO PU-PEG hydrogel, the formulation with the highest PU-PEG content, displaying low protein adsorption.

The fact that albumin (globular shape) adsorption is higher than fibrinogen (elongated rod-like shape) might be due to the relative size of the proteins. Since fibrinogen is larger than albumin it may

have a lower ability to diffuse into the hydrogel. A similar result was found with silicone surfaces coated with niobium pentoxide and a monolayer composed of different PEG densities, in which higher PEG density exhibited more adsorption of smaller proteins (such as albumin, 67kDa) in relation to larger proteins (such as fibrinogen, 340kDa) [60]. Previous studies have also reported that higher PEG content can inversely influence the amount of protein adsorbed for both albumin and fibrinogen, and can have an effect on protein orientation on an uncharged PEG grafted phospholipid monolayer. Nonetheless the structure of both negatively charged proteins, is preserved when adsorbed onto this surface, not influencing the protein adsorption process [59].

Protein adsorption, *in vitro* and *in vivo*, of inflammatory-related proteins has been shown in PEG-based hydrogels being a key characteristic to facilitate cellular adhesion of macrophages. Such plays a critical role in the mediation of the FBR, known to be initiated by protein adsorption onto the materials [58]. Curiously, no correlation of protein absorption and cell adhesion results was observed in the present work where higher protein adsorption of PU-PEG hydrogels and PDMS did not necessarily correlate with a higher adhered cell density.

The values for cell attachment measurements (Figure 3.13), were obtained by two different methods, where cell count per hydrogel surface area, appears to be the best method of cell count, when compared to the cell count per area of each counted square, since it allows for quantification of the largest area possible instead of squared sections of parts of the surface that might not be as representative. Regardless of this, assessing the cell number directly form the hydrogel surface does have some disadvantages such as not being possible to count by naked eye when cell number is too high.

One hypothesis as to why cellular adhesion was lower than expected might be that the hydrogels surface does not allow or provide good surface adherence. Even though adsorption of serum proteins was promoted by incubating the gels in medium, and only after the cells were added to the culture, the cells cannot attach and are not able to survive. Such might be due to the PU-PEG hydrogels nonfouling behavior, often associated with PEG's hydrophilic nature. This is in line with previous studies on a PU-based hydrogel that, when synthesized with PEG, also demonstrated a lower number of cells adhered to the materials surface [34].

Both comparable protein adsorption to PDMS and low cellular attachment are indicators of the PU-PEG hydrogels non-fouling properties. This could further be an early indication of the anti-FBR behavior of the hydrogels, that could be studied by implanting the PU-PEG hydrogel subcutaneously in animal models [58]. As no hydrogel degradation was shown through the duration of the degradation study, compatible with the timeline for the evolution of the FBR until encapsulation of the biomaterial, the measurement of the FBR could be assessed. Such is usually performed by tracking the fibrous capsule formation and immune inflammatory cell infiltration by immunohistochemistry following the implantation of the hydrogels, during different time-points to cover its full-time course [54].

Moreover, this PU-PEG hydrogels could present additional applications in tissue engineering and regenerative medicine. The varied mechanical properties make the materials potentially applicable to a

wider range of tissue and organ applications within tissue engineering, as well as with further investigation their capacity as a drug delivery vehicle or their potential to decrease the FBR could possibly be explored.

4.1. Conclusion

In conclusion, by using different PU-PEG hydrogel formulations it was possible to study how each one of them responded to the same range of mechanical forces and strains. The PU-PEG hydrogels rheological properties varied according to the PU-PEG content, with higher mechanical strength displayed in hydrogels with higher PU-PEG content, presenting compatible values with previous studied measurements for tissues and hydrogels for wound healing. Contrary to the mechanical properties, the swelling behavior of the hydrogels showed higher swelling ratios when the PU-PEG content was the lowest. The substitution of the DABCO catalyst for the DBTDL catalyst did not affect the mechanical properties of the gel. The major effect of the change in the catalyst is seen in the cytotoxicity assays where, due to the retention of tin in the hydrogels network, the 23% (w/v) DBTDL PU-PEG Vial hydrogel had a negative effect on cell survival. Thus, providing valuable information on the impact of using DBTDL as a catalyst, and highlighting the benefit of using DABCO in the overall synthetic process due to its improved biocompatibility. Both protein adsorption and cell adhesion studies contributed to the characterization of the potential nonfouling properties of these PU-PEG hydrogels. By comparing them against a highly used standard biomaterial, PDMS, the hydrogels displayed comparable protein adsorption, as well as low cell adhesion. This work unveiled PU-PEG hydrogels' potential as material for wound healing and demonstrated other desirable characteristics that could make the material appropriate for broader applications in tissue engineering and regenerative medicine.

BIBLIOGRAPHY

1 Dzobo, K. *et al.* Advances in Regenerative Medicine and Tissue Engineering: Innovation and Transformation of Medicine. *Stem Cells Int* **2018**, 1-24, doi:10.1155/2018/2495848 (2018).

2 Howard, D., Buttery, L. D., Shakesheff, K. M. & Roberts, S. J. Tissue engineering: strategies, stem cells and scaffolds. *J Anat* **213**, 66-72, doi:10.1111/j.1469-7580.2008.00878.x (2008).

3 O'Brian, F. J. Biomaterials & scaffolds for tissue engineering. *Materials Today* **14**, 88-95, doi:10.1016/S1369-7021(11)70058-X (2011).

4 Ratner, B. D. Biomaterials: Been There, Done That, and Evolving into the Future. *Annu Rev Biomed Eng* **21**, 171-191, doi:10.1146/annurev-bioeng-062117-120940 (2019).

5 Mariani, E., Lisignoli, G., Borzì, R. M. & Pulsatelli, L. Biomaterials: Foreign Bodies or Tuners for the Immune Response? *Int J Mol Sci* **20**, 1-42, doi:10.3390/ijms20030636 (2019).

6 Reddy, M. S. B., Ponnamma, D., Choudhary, R. & Sadasivuni, K. K. A Comparative Review of Natural and Synthetic Biopolymer Composite Scaffolds. *Polymers (Basel)* **13**, 1-51, doi:10.3390/polym13071105 (2021).

7 Mogoşanu, G. D. & Grumezescu, A. M. Natural and synthetic polymers for wounds and burns dressing. *Int J Pharm* **463**, 127-136, doi:10.1016/j.ijpharm.2013.12.015 (2014).

8 Kohane, D. S. & Langer, R. Polymeric biomaterials in tissue engineering. *Pediatr Res* **63**, 487-491, doi:10.1203/01.pdr.0000305937.26105.e7 (2008).

9 Mir, M. *et al.* Synthetic polymeric biomaterials for wound healing: a review. *Prog Biomater* **7**, 1-21, doi:10.1007/s40204-018-0083-4 (2018).

10 Gunatillake, P., Mayadunne, R. & Adhikari, R. Recent developments in biodegradable synthetic polymers. *Biotechnol Annu Rev* **12**, 301-347, doi:10.1016/S1387-2656(06)12009-8 (2006).

11 Teo, A. J. T. *et al.* Polymeric Biomaterials for Medical Implants and Devices. *ACS Biomater Sci Eng* **2**, 454-472, doi:10.1021/acsbiomaterials.5b00429 (2016).

12 Whitaker, R., Hernaez-Estrada, B., Hernandez, R. M., Santos-Vizcaino, E. & Spiller, K. L. Immunomodulatory Biomaterials for Tissue Repair. *Chem Rev* **121**, 11305-11335, doi:10.1021/acs.chemrev.0c00895 (2021).

13 Maitz, M. F. Applications of synthetic polymers in clinical medicine. *Biosurface and Biotribology* **1**, 161-176, doi:10.1016/j.bsbt.2015.08.002 (2015).

14 Chandorkar, Y., K, R. & Basu, B. The Foreign Body Response Demystified. *ACS Biomater Sci Eng* **5**, 19-44, doi:10.1021/acsbiomaterials.8b00252 (2019).

15 Veiseh, O. & Vegas, A. J. Domesticating the foreign body response: Recent advances and applications. *Adv Drug Deliv Rev* **144**, 148-161, doi:10.1016/j.addr.2019.08.010 (2019).

16 Zhou, G. & Groth, T. Host Responses to Biomaterials and Anti-Inflammatory Design-a Brief Review. *Macromol Biosci* **18**, 1-15, doi:10.1002/mabi.201800112 (2018).

17 Zhang, D. *et al.* Dealing with the Foreign-Body Response to Implanted Biomaterials: Strategies and Applications of New Materials. *Advanced Functional Materials* **31**, 1-22, doi:10.1002/adfm.202007226 (2020).

18 Zhang, H. & Chiao, M. Anti-fouling Coatings of Poly(dimethylsiloxane) Devices for Biological and Biomedical Applications. *J Med Biol Eng* **35**, 143-155, doi:10.1007/s40846-015-0029-4 (2015).

19 Zhang, A., Cheng, L., Hong, S., Yang, C. & Lin, Y. Preparation of anti-fouling silicone elastomers by covalent immobilization of carboxybetaine. *RSC Adv.* **5**, 88456-88463, doi:10.1039/C5RA17206C (2015).

20 Wipff, P. J. *et al.* The covalent attachment of adhesion molecules to silicone membranes for cell stretching applications. *Biomaterials* **30**, 1781-1789, doi:10.1016/j.biomaterials.2008.12.022 (2009).

21 Chuah, Y. J. *et al.* Simple surface engineering of polydimethylsiloxane with polydopamine for stabilized mesenchymal stem cell adhesion and multipotency. *Sci Rep* **5**, 1-12, doi:10.1038/srep18162 (2015).

22 Doloff, J. C. *et al.* The surface topography of silicone breast implants mediates the foreign body response in mice, rabbits and humans. *Nat Biomed Eng* **5**, 1115-1130, doi:10.1038/s41551-021-00739-4 (2021).
23 Su, J., Li, J., Liang, J. & Zhang, K. Hydrogel Preparation Methods and Biomaterials for Wound Dressing. *Life (Basel)* **11**, 1-22, doi:10.3390/life11101016 (2021).
24 Kim, J. K. *et al.* Natural and synthetic biomaterials for controlled drug delivery. *Arch Pharm Res* **37**, 60-68, doi:10.1007/s12272-013-0280-6 (2014).
25 Gupta, A. *et al.* The production and application of hydrogels for wound management: A review. *European Polymer Journal* **111**, 134-151, doi:10.1016/j.eurpolymj.2018.12.019 (2019).
26 Chen, S. L. *et al.* A PEG-Based Hydrogel for Effective Wound Care Management. *Cell Transplant* **27**, 275-284, doi:10.1177/0963689717749032 (2018).
27 Liu, S. *et al.* Injectable and Degradable PEG Hydrogel with Antibacterial Performance for Promoting Wound Healing. *ACS Applied Bio Materials* **4**, 2769-2780, doi:10.1021/acsabm.1c00004 (2021).
28 Lin, Y. J. *et al.* Stimulation of wound healing by PU/hydrogel composites containing fibroblast growth factor-2. *J Mater Chem B* **3**, 1931-1941, doi:10.1039/c4tb01638f (2015).
29 Kamaci, M. Polyurethane-based hydrogels for controlled drug delivery applications. *European Polymer Journal* **123**, 1-11, doi:https:10.1016/j.eurpolymj.2019.109444 (2020).
30 Castel, N., Soon-Sutton, T., Deptula, P., Flaherty, A. & Parsa, F. D. Polyurethane-coated breast implants revisited: a 30-year follow-up. *Arch Plast Surg* **42**, 186-193, doi:10.5999/aps.2015.42.2.186 (2015).
31 Dhivya, S., Padma, V. & Santhini, E. Wound dressings - a review. *Biomedicine (Taipei)* **5**, 24-28, doi:10.7603/s40681-015-0022-9 (2015).
32 Petrini, P., Farè, S., Piva, A. & Tanzi, M. C. Design, synthesis and properties of polyurethane hydrogels for tissue engineering. *J Mater Sci Mater Med* **14**, 683-686, doi:10.1023/a:1024955531173 (2003).
33 Divakaran, A., Torris, A., Lele, A. & Badiger, M. Porous poly(ethylene glycol)–polyurethane hydrogels as potential biomaterials. *Polymer International* **64**, 397-404, doi:10.1002/pi.4802 (2014).
34 Zhang, C., Zhang, N. & Wen, X. Synthesis and characterization of biocompatible, degradable, light-curable, polyurethane-based elastic hydrogels. *J Biomed Mater Res A* **82**, 637-650, doi:10.1002/jbm.a.30992 (2007).
35 Li, J., Ma, L., Chen, G., Zhou, Z. & Li, Q. A high water-content and high elastic dual-responsive polyurethane hydrogel for drug delivery. *J Mater Chem B* **3**, 8401-8409, doi:10.1039/c5tb01702e (2015).
36 Rao, L., Zhou, H., Li, T., Li, C. & Duan, Y. Y. Polyethylene glycol-containing polyurethane hydrogel coatings for improving the biocompatibility of neural electrodes. *Acta Biomater* **8**, 2233-2242, doi:10.1016/j.actbio.2012.03.001 (2012).
37 Yoo, H. J. & Kim, H. D. Synthesis and properties of waterborne polyurethane hydrogels for wound healing dressings. *J Biomed Mater Res B Appl Biomater* **85**, 326-333, doi:10.1002/jbm.b.30950 (2008).
38 Tottoli, E. M. *et al.* Skin Wound Healing Process and New Emerging Technologies for Skin Wound Care and Regeneration. *Pharmaceutics* **12**, 1-30, doi:10.3390/pharmaceutics12080735 (2020).
39 Saghazadeh, S. *et al.* Drug delivery systems and materials for wound healing applications. *Adv Drug Deliv Rev* **127**, 138-166, doi:10.1016/j.addr.2018.04.008 (2018).
40 Boateng, J. S., Matthews, K. H., Stevens, H. N. & Eccleston, G. M. Wound healing dressings and drug delivery systems: a review. *J Pharm Sci* **97**, 2892-2923, doi:10.1002/jps.21210 (2008).
41 Gosain, A. & DiPietro, L. A. Aging and wound healing. *World J Surg* **28**, 321-326, doi:10.1007/s00268-003-7397-6 (2004).
42 Guo, S. & Dipietro, L. A. Factors affecting wound healing. *J Dent Res* **89**, 219-229, doi:10.1177/0022034509359125 (2010).
43 Winter, G. D. Formation of the scab and the rate of epithelization of superficial wounds in the skin of the young domestic pig. *Nature* **193**, 293-294, doi:10.1038/193293a0 (1962).

44 Murray, R. Z., West, Z. E., Cowin, A. J. & Farrugia, B. L. Development and use of biomaterials as wound healing therapies. *Burns Trauma* **7**, 1-9, doi:10.1186/s41038-018-0139-7 (2019).
45 Piraino, F. & Selimović, Š. A Current View of Functional Biomaterials for Wound Care, Molecular and Cellular Therapies. *Biomed Res Int* **2015**, 1-10, doi:10.1155/2015/403801 (2015).
46 Müller, A., Wapler, M. C. & Wallrabe, U. A quick and accurate method to determine the Poisson's ratio and the coefficient of thermal expansion of PDMS. *Soft Matter* **15**, 779-784, doi:10.1039/c8sm02105h (2019).
47 Glover, J. D., McLaughlin, C. E., McFarland , M. K. & Pham, J. T. Extracting uncrosslinked material from low modulus sylgard 184 and the effect on mechanical properties. *Journal of Polymer science* **58**, 343-351, doi:10.1002/pol.20190032 (2020).
48 Holt, B., Tripathi, A. & Morgan, J. Viscoelastic response of human skin to low magnitude physiologically relevant shear. *J Biomech* **41**, 2689-2695, doi:10.1016/j.jbiomech.2008.06.008 (2008).
49 Geerligs, M., Peters, G. W., Ackermans, P. A., Oomens, C. W. & Baaijens, F. P. Linear viscoelastic behavior of subcutaneous adipose tissue. *Biorheology* **45**, 677-688, doi:10.3233/BIR-2008-0517(2008).
50 Guimarães, C. F., Gasperini, L., Marques, A. P. & Reis, R. L. The stiffness of living tissues and its implications for tissue engineering. *Nature Reviews Materials* **5**, 351–370, doi:10.1038/s41578-019-0169-1 (2020).
51 Lee, J. *et al.* In Situ Hydrogel-Forming/Nitric Oxide-Releasing Wound Dressing for Enhanced Antibacterial Activity and Healing in Mice with Infected Wounds. *Pharmaceutics* **11**, 1-18, doi:10.3390/pharmaceutics11100496 (2019).
52 Zhao, Y. *et al.* Transparent Conductive Supramolecular Hydrogels with Stimuli-Responsive Properties for On-Demand Dissolvable Diabetic Foot Wound Dressings. *Macromol Rapid Commun* **41**, 1-11, doi:10.1002/marc.202000441 (2020).
53 Kokabi, M., Sirousazar, M. & Hassan, Z. M. PVA–clay nanocomposite hydrogels for wound dressing. *European Polymer Journal* **43**, 773-781, doi:10.1016/j.eurpolymj.2006.11.030 (2007).
54 Lynn, A. D., Kyriakides, T. R. & Bryant, S. J. Characterization of the in vitro macrophage response and in vivo host response to poly(ethylene glycol)-based hydrogels. *J Biomed Mater Res A* **93**, 941-953, doi:10.1002/jbm.a.32595 (2010).
55 Tanzi, M. C. *et al.* Cytotoxicity of some catalysts commonly used in the synthesis of copolymers for biomedical use. *Journal of Materials Science: Materials in Medicine* **5**, 393-396, doi:10.1007/BF00058971 (1994).
56 Merinas-Amo, R., Martínez-Jurado, M., Jurado-Güeto, S., Alonso-Moraga, Á. & Merinas-Amo, T. Biological Effects of Food Coloring in In Vivo and In Vitro Model Systems. *Foods* **8**, 1-19, doi:10.3390/foods8050176 (2019).
57 Riedel, T. *et al.* Complete identification of proteins responsible for human blood plasma fouling on poly(ethylene glycol)-based surfaces. *Langmuir* **29**, 3388-3397, doi:10.1021/la304886r (2013).
58 Swartzlander, M. D. *et al.* Linking the foreign body response and protein adsorption to PEG-based hydrogels using proteomics. *Biomaterials* **41**, 26-36, doi:10.1016/j.biomaterials.2014.11.026 (2015).
59 Bernhard, C. *et al.* Repelling and ordering: the influence of poly(ethylene glycol) on protein adsorption. *Phys Chem Chem Phys* **19**, 28182-28188, doi:10.1039/c7cp05445a (2017).
60 Michel, R., Pasche, S., Textor, M. & Castner, D. G. Influence of PEG architecture on protein adsorption and conformation. *Langmuir* **21**, 12327-12332, doi:10.1021/la051726h (2005).

2021

INÊS ISABEL PEREIRA CORREIA

POLYURETHANE – POLY(ETHYLENE GLYCOL) HYDROGELS FOR TISSUE ENGINEERING APPLICATIONS

NOVA SCHOOL OF SCIENCE & TECHNOLOGY